

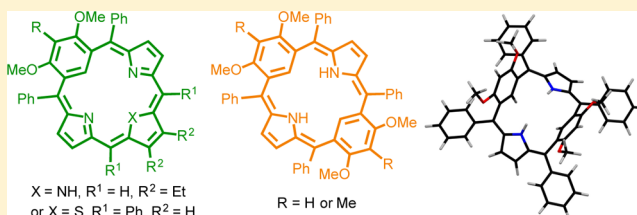
Synthesis and Metalation of Dimethoxybenzporphyrins, Thiabenzporphyrins, and Dibenzporphyrins

Stacy C. Fosu, Gregory M. Ferrence, and Timothy D. Lash*

Department of Chemistry, Illinois State University, Normal, Illinois 61790-4160, United States

Supporting Information

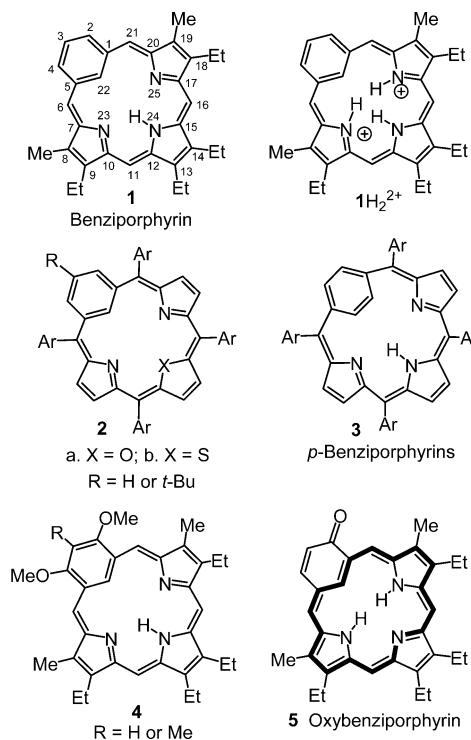
ABSTRACT: Dimethoxybenztripyrans were prepared in excellent yields by reacting benzene dicarbinols with $\text{BF}_3 \cdot \text{Et}_2\text{O}$ and excess pyrrole in refluxing 1,2-dichloroethane. Reaction with a pyrrole dialdehyde in the presence of TFA, followed by oxidation with DDQ, afforded good yields of *meso*-diphenyl-dimethoxybenzporphyrins. These dimethoxybenzporphyrinoids exhibited weakly diatropic properties that were enhanced upon protonation. The dimethoxybenztripyrans also reacted with a thiophene dicarbinol to give dimethoxythiabenzporphyrins, and the nonplanar nature of this system was demonstrated by X-ray crystallography. The dimethoxybenzporphyrins reacted with palladium(II) acetate to give the related organometallic derivatives, but the thiabenzporphyrins underwent a demethylation to afford palladium(II) thiaoxybenzporphyrins. Related palladium(II) complexes were also prepared from previously reported thiabenzporphyrinoids. The X-ray structure for one of the complexes showed that the six-membered ring is very distorted and the thiophene ring is strongly tilted out of the plane of the macrocycle. The dimethoxybenztripyrans also reacted with dimethoxybenzene dicarbinols to give the first examples of dibenzporphyrins, thereby further demonstrating the versatility of this synthetic methodology.



INTRODUCTION

Benzporphyrins **1**, porphyrin analogues with a 1,3-phenylene moiety replacing one of the pyrrole subunits, have attracted considerable attention^{1,2} since they were first described in the 1990s.^{1,3,4} Syntheses of *meso*-tetraarylbenzporphyrins **2** were subsequently developed,^{5,6} as well as *p*-benzporphyrins **3**, which possess a 1,4-phenylene subunit.⁷ The metalation of benzporphyrins has been widely investigated, and the system affords organometallic derivatives with nickel(II), palladium(II), and platinum(II) salts.^{5,8,9} In addition, selective oxidation reactions at the internal carbon have been described,^{5,10} and an oxidative metalation with copper(II) chloride has been reported.¹¹ Dihydrobenzporphyrins have been shown to have promise as fluorescence detectors for zinc cations¹² and have been incorporated into multidimensional nanostructure arrays.¹³ The benzporphyrin system is nonaromatic,¹ although upon protonation the macrocycle forms a dication, 1H_2^{2+} , that takes on a small amount of diatropic character.^{6,9,14} The presence of an electron-donating *tert*-butyl substituent slightly enhanced the diatropicity of the dications,⁶ and methoxy groups (e.g., for benzporphyrins **4**) appear to imbue the free base with a degree of diatropic character that is greatly enhanced upon protonation.^{14,15} The introduction of a 2-hydroxy substituent triggers a keto–enol-like tautomerization to form a fully aromatic system known as oxybenzporphyrin (**5**),^{5,16} and further modified highly diatropic systems are also known.¹⁷ In addition, related naphthoporphyrins⁹ and azabenzporphyrins (pyriporphyrins)^{18,19} have been reported.

Despite the many efforts expended on the synthesis and investigation of benzporphyrins, it was not until 2013 that the



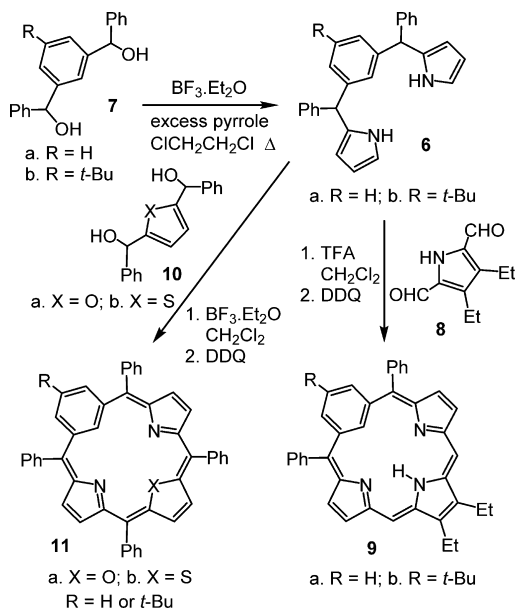
first examples of heterobenzporphyrins were reported.²⁰ Tripyrane analogues **6** were prepared in good yields by

Received: September 6, 2014

Published: October 16, 2014

reacting the known carbinols **7**⁶ with excess pyrrole in the presence of boron trifluoride etherate (Scheme 1). The

Scheme 1

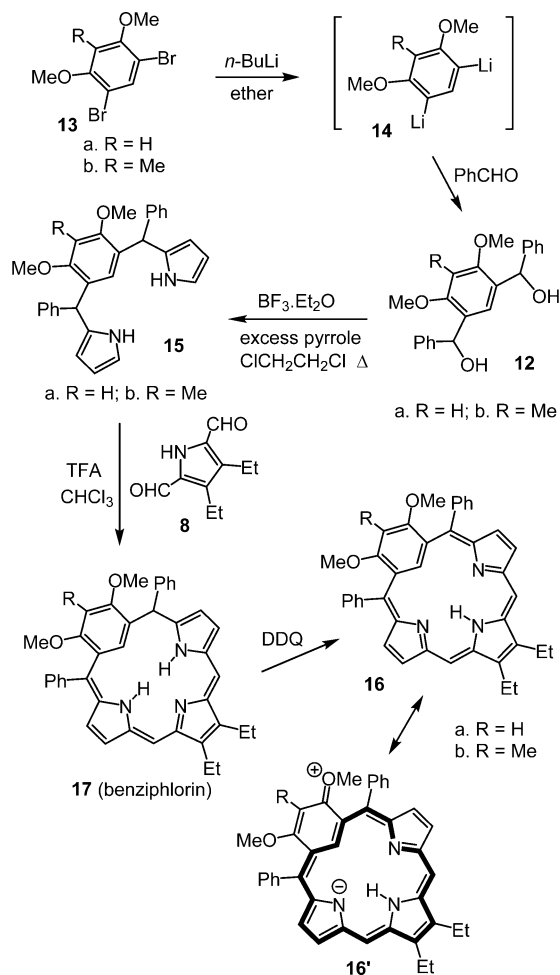


tripyrans reacted with pyrrole dialdehyde **8** in the presence of trifluoroacetic acid in dichloromethane, followed by oxidation with DDQ, to give the *meso*-diphenylbenzporphyrins **9**. Alternatively, condensation with furan or thiophene dicarbinols **10** and boron trifluoride etherate, followed by oxidation with DDQ, gave heterobenziporphyrins **11a** and **11b**.²⁰ The new porphyrinoids **11** exhibited no overall diatropic character but, like regular benziporphyrins, showed the emergence of a diamagnetic ring current in the presence of acid.²⁰ The small number of steps required to prepare porphyrinoids of this type makes this approach very appealing. With this in mind, we targeted the synthesis of dimethoxybenziporphyrins and related thiabenziporphyrins using the benzitripyrrane strategy. This approach has not only made these new porphyrinoids accessible but has also enabled the preparation of novel palladium(II) derivatives. In addition, the same methodology can be used to prepare hitherto unknown dibenziporphyrins.²¹

RESULTS AND DISCUSSION

Diphenyldimethoxybenzporphyrins. Dicarbinols **12** were prepared 62–71% yield by treating dibromodimethoxybenzenes **13** with *n*-butyllithium, followed by reacting the intermediary dilithiated species **14** with benzaldehyde (Scheme 2).¹⁵ The dicarbinols were dissolved with a large excess of pyrrole in 1,2-dichloroethane, catalytic boron trifluoride etherate was added, and the mixture was stirred under reflux overnight. The excess pyrrole was removed under vacuum, and the residues were purified by column chromatography on silica gel, eluting with a 60:40 mixture of hexanes and dichloromethane containing 1% triethylamine. The pure benzitripyrranes **15** were isolated as mixtures of diastereoisomers in 81–90% yield. Tripyrrane analogues **15** were reacted with pyrrole dialdehyde **8** and TFA for 2 h and then treated with 1 equiv of DDQ for a further 1 h. The best results were obtained when chloroform was used as the reaction solvent. Column

Scheme 2



chromatography on grade 3 alumina afforded a dark green band corresponding to the desired benziporphyrins **16**, but an initial blue band was also noted due to the presence of the related phlorins **17**. Condensation of **15** with **8** initially gives rise to benziphlorins **17**, and an oxidation step is required to form the fully conjugated porphyrinoids **16**. In the case of **17a**, the benziphlorin proved to be too unstable to fully characterize, but methyl-substituted phlorin **17b** was more robust and was isolated in 10% yield. The spectroscopic properties for **17b** were consistent with an asymmetrical nonaromatic system, and the *meso*-protons gave rise to two ¹H singlets in the proton NMR spectrum at 5.77 and 6.04 ppm. The internal CH proton afforded a singlet at 6.41 ppm, which is consistent with expectations for an electron-rich aromatic ring. The benziporphyrin products **16a** and **16b** were isolated as dark green solids in 42% and 69% yields, respectively. The proton NMR spectrum for benziporphyrin **16a** indicated that the macrocycle is weakly diatropic. The *meso*-protons at positions 11 and 16 gave rise to a singlet at 6.27 ppm, while the internal 22-H appeared slightly upfield at 5.95 ppm. However, in the proton NMR spectrum of **16b**, the *meso*-protons appeared at 6.10 ppm (2H), while the 22-H gave a singlet at 6.43 ppm, values that suggest that much of the diatropic character has been lost. The aromatic properties of dimethoxybenziporphyrins have been attributed to the presence of dipolar resonance contributors such as **16'** that possess 18 π electron delocalization pathways.^{14,22} These interactions diminish the aromatic properties

of the arene unit and require charge delocalization, so their contributions are somewhat limited. This type of conjugation is more favorable for **16a** than for **16b**, as the latter species has a methyl group placed between the two methoxy moieties.¹⁴ In order for the methoxy substituents to be electron-donating, the oxygens have to take on sp^2 character, and this necessitates placing the OMe groups in the plane of the macrocycle. Clearly, this type of interaction is sterically hindered in the case of **16b**. The proton and carbon-13 NMR spectra of benziporphyrins **16** confirm the presence of a plane of symmetry. The UV-vis spectrum for **16a** in 1% triethylamine–chloroform gave a medium intensity Soret-like band at 423 nm and broad absorptions at higher wavelengths (Figure 1). For **16b**, the

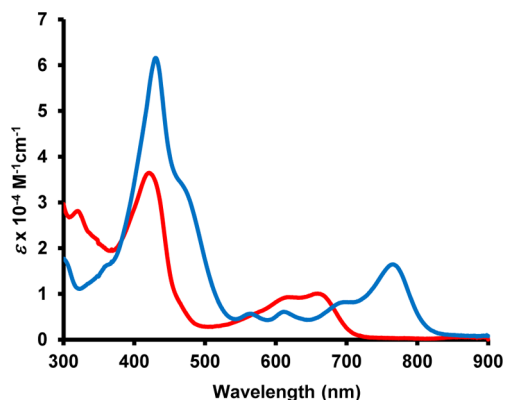
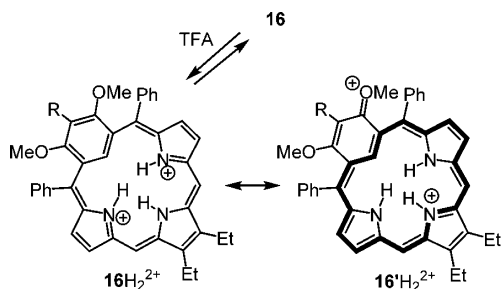


Figure 1. UV-vis spectra of dimethoxybenziporphyrin **16a** in 1% triethylamine–chloroform (free base, red line) and 1% TFA–chloroform (dication $16aH_2^{2+}$, blue line).

Soret-like band shifted to 409 nm. As expected, addition of TFA to solutions of **16** afforded diprotonated species that showed significantly increased diatropic characteristics (Scheme 3). The proton NMR spectrum of $16aH_2^{2+}$ in TFA– $CDCl_3$

Scheme 3

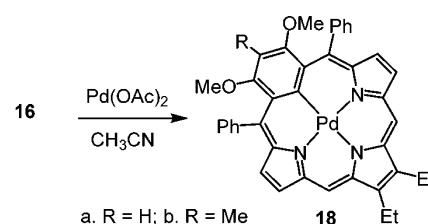


gave a 2H singlet for the *meso*-protons at 7.27 ppm, while the pyrrolic hydrogens afforded two 2H doublets of doublets at 7.56 and 7.95 ppm (the splitting is due in part to transannular coupling by the NH protons). The observed downfield shifts are consistent with the presence of a diamagnetic ring current, and this is further supported by the upfield shift observed for the 22-H which appears as a singlet at 3.77 ppm. The diatropic nature of the dication can be attributed to resonance contributors such as $16a'H_2^{2+}$ that aid in charge delocalization. These effects are substantially reduced for $16bH_2^{2+}$ in TFA– $CDCl_3$, and for this species the *meso*-protons appeared as a 2H singlet at 6.90 ppm, while the internal CH gave a resonance at 5.07 ppm. This difference can again be ascribed to the methyl

group sterically disrupting electronic interactions with the methoxy substituents. The UV-vis spectrum for $16a'H_2^{2+}$ in 1% TFA–chloroform showed a stronger Soret-like band at 430 nm and a series of broadened absorptions at higher wavelengths culminating in a medium intensity band at 765 nm (Figure 1). Similarly, the UV-vis spectrum of $16bH_2^{2+}$ gave a Soret-like absorption at 442 nm and a medium-sized absorption at 774 nm.

The metalation of benziporphyrins **16a,b** was also briefly investigated.²³ Specifically, **16a** and **16b** were reacted with palladium(II) acetate in refluxing acetonitrile, and following purification by column chromatography and recrystallization from chloroform–methanol, the organometallic products **18** were isolated as deep purple crystals in 58% and 65% yields, respectively (Scheme 4). The UV-vis spectrum for palladium

Scheme 4



complex **18a** gave a Soret band at 448 nm and a series of Q bands between 500 and 800 nm (Figure 2). The UV-vis

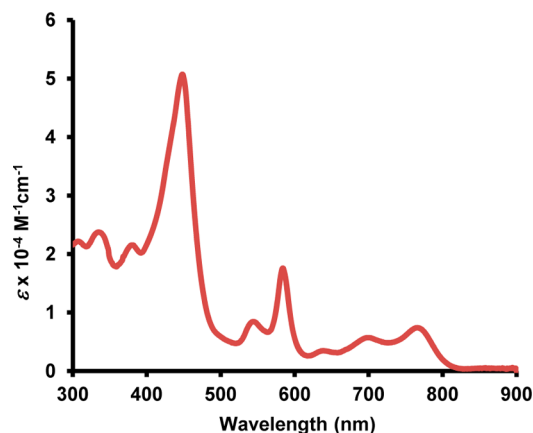


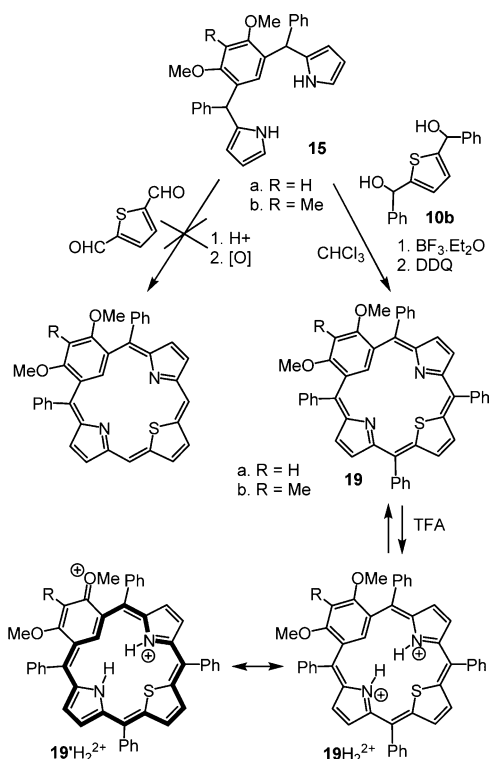
Figure 2. UV-vis spectrum of palladium(II) dimethoxybenziporphyrin **18a** in chloroform.

spectrum of **18b** also afforded a Soret-like band at 440 nm, but the higher wavelength Q bands were weaker and far more broadened in this case. In the proton NMR spectrum for **18a** in $CDCl_3$, the *meso*-protons afforded a 2H singlet at 7.73 ppm, while the pyrrolic protons gave rise to a 2H doublet at 7.84 ppm and an obscured resonance that overlaps with the *o*-phenyl protons at 7.66 ppm. These values are significantly downfield from those observed for the free base form of **16a**, and the results imply the presence of a moderate diamagnetic ring current in the palladium(II) derivative. This effect may be due in part to the macrocycle taking on a more planar conformation. The steric interactions between the *meso*-phenyl substituents and the methoxy groups in **16** are likely to lead to significant distortions, but the coordinated palladium(II) will draw the individual rings together. For **18b**, the *meso*-protons show up at 7.30 ppm, and the pyrrole protons are present at

7.41 and 7.69 ppm. The decreased downfield shifts in this case can again be attributed to the disruptive influence of the methyl substituent.

Dimethoxythiabenziporphyrins. Attempts to condense 2,5-thiophenedicarbaldehyde with benzitripyranes **15** failed to give any isolatable thiabenziporphyrin products (Scheme 5).

Scheme 5



However, when thiophene dicarbinol **10b**²⁴ was reacted with **15** and boron trifluoride etherate in chloroform at room temperature and then oxidized with DDQ, the corresponding tetraphenylthiabenziporphyrins **19** were isolated as dark blue-green powders in 38–41% yield (Scheme 5). The proton NMR spectrum for **19a** showed the inner CH at 6.34 ppm, compared to a value of 7.22 ppm seen for thiabenziporphyrin **11b** (R = H).²⁰ The 3-methyldimethoxythiabenziporphyrin **19b** gave an intermediary value of 6.67 ppm. These results indicate the presence of a very weak diatropic ring current that has been induced by the two methoxy groups, but the effect is very small possibly due in part to the nonplanar nature of these macrocycles (see below). Proton and carbon-13 NMR spectroscopy confirmed the presence of a macrocyclic plane of symmetry, and the identity of these porphyrinoids was further supported by high-resolution EI MS. The UV–vis spectrum for **19a** in 1% triethylamine–chloroform was nondescript, showing two medium intensity bands at 346 and 437 nm and a weaker broad absorption near 600 nm (Figure 3). A similar UV–vis spectrum was observed for **19b**. The benziporphyrinoid structures **19a** and **19b** were optimized using B3LYP-6-311++G**, and these calculations demonstrated that these porphyrinoids are nonplanar with the benzene ring pivoted from the mean macrocyclic plane by 58.18° and 65.33° for **19a** and **19b**, respectively (Table 1). Figure 4 shows the geometry optimized conformation for thiabenziporphyrin **19a**. In order to further assess the diatropic characteristics of

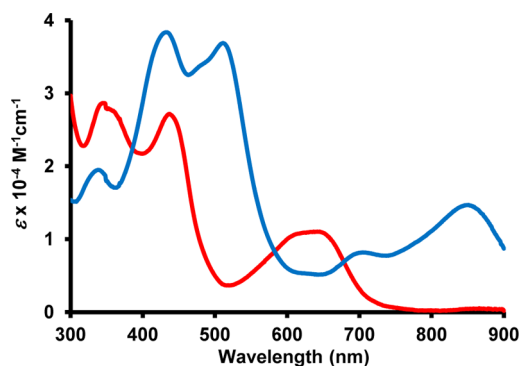


Figure 3. UV–vis spectra of thiabenziporphyrin **19a** in 1% triethylamine–chloroform (free base, red line) and 1% TFA–chloroform (dication **19aH**₂²⁺, blue line).

Table 1. Angles (deg) between the Planes of Each Individual Ring and the Overall Plane of Macrocycles **19a,b** and **32a–c**^a

molecule	a	b	c	d
19a	58.18	29.91	0.91	29.91
19b	65.33	29.26	0.51	29.27
32a	63.94	37.89	63.94	37.89
32b	69.41	38.43	69.41	38.43
32c	70.46	38.21	63.40	38.21

^aFor the assignments of rings a, b, c, and d, see Table 2.

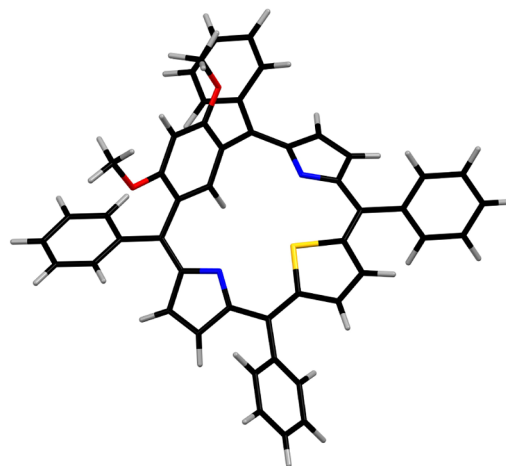
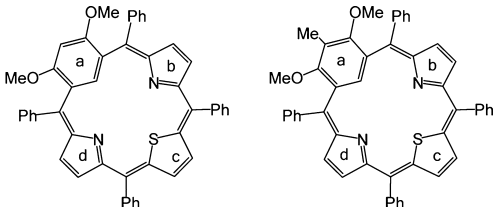


Figure 4. DFT-calculated conformation for thiabenziporphyrin **19a**.

the thiabenziporphyrins, nucleus-independent chemical shift (NICS) values²⁵ were computed for the center of the macrocycle as well as the center of each individual ring (Table 2). Porphyrinoids **19a** and **19b** gave NICS(0) values of −1.82 and −1.85, suggesting that these macrocycles possess only a trace amount of diatropic character in agreement with the NMR data. The benzene subunits give typical aromatic values, but the remaining subunits show only a small degree of diatropicity.

Tetraphenylthiabenziporphyrin **19b** was also characterized by X-ray diffraction analysis (Figure 5), and this both confirms the presence of a thiabenziporphyrin framework and demonstrates that the macrocycle deviates substantially from planarity as evidenced by the 0.798 Å rms distance the framework atoms lie from the core plane defined by C22, N23, S24, and N25. Of the 25 framework atoms, 7 deviate more than 1.00 Å from this

Table 2. Calculated NICS Values (ppm) for Thiabenziporphyrins 19a and 19b



molecule	19a	19b
NICS (0)	−1.82	−1.85
NICS (a)	−8.05	−10.25
NICS (b)	−1.54	−1.56
NICS (c)	−2.99	−2.55
NICS (d)	−1.54	−1.56

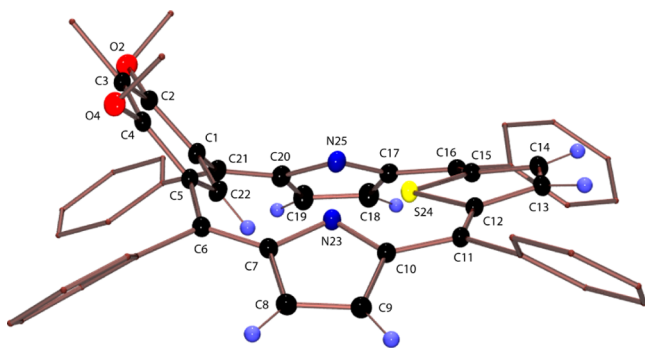
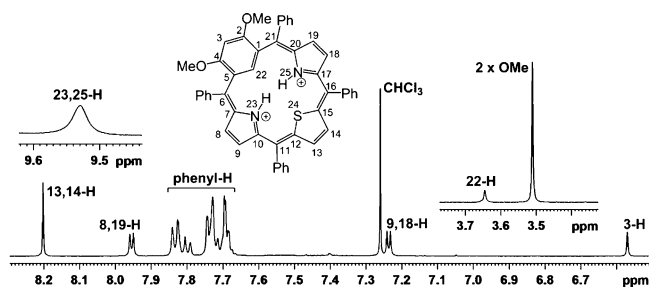


Figure 5. Color POV-Ray rendered ORTEP III drawing (50% probability level, selected hydrogen atoms omitted for clarity) of compound 19b.

plane. The macrocycle may be described as saddled with C3 at the horn. So defined, the framework arene ring tilts $49.86(2)^\circ$ relative to the core plane with C2 (1.501(1) Å), C3 (2.123(1) Å), and C4 (1.617(1) Å) rising above the plane. This tilt is slightly reduced compared to the value obtained in the DFT calculations, but the difference may be due to crystal packing forces. The pyrrolic rings adjacent to the framework arene ring tilt $30.24(4)^\circ$ and $32.47(3)^\circ$ relative to the core plane, with C8 (1.072(1) Å), C9 (1.110(1) Å), C18 (1.144(1) Å), and C19 (1.192(1) Å) falling below the plane. The thiophene ring opposite to the framework arene ring tilts $6.62(2)^\circ$ relative to the core plane, with C13 (0.305(1) Å) and C14 (0.348(1) Å) rising a little above the plane. The larger tilt of the arene ring is attributable to steric repulsion between the C2 and C4 attached methoxy substituents and the *meso*-phenyl substituents. The phenyl groups are, in fact, canted $33.10(3)^\circ$ and $29.20(3)^\circ$ relative to the core plane. The structure exhibits framework bond distances consistent with a generally localized π -bonding model. The longest C–C bonds in the framework are C1–C21 (1.484(1) Å) and C5–C6 (1.481(1) Å). The significant single bond character of these bonds may facilitate the substantial deformation from coplanarity of the dimethoxymethylbenzene ring with the main macrocycle.

Addition of TFA to solutions of **19** gave the corresponding dication **19H₂²⁺** (Scheme 5), and these diprotonated species showed enhanced diatropic characteristics (Figure 6). Although thiabenziporphyrin dication **11bH₂²⁺** also show a small diamagnetic ring current (Table 3), the upfield shift to the inner CH is increased from 5.29 ppm for **11bH₂²⁺** to 3.65 ppm

Figure 6. 500 MHz proton NMR spectrum of thiabenziporphyrin dication **19aH₂²⁺** in TFA–CDCl₃.Table 3. Selected Chemical Shifts (ppm) for the Proton NMR Spectra of Thiabenziporphyrin Cations **11bH₂²⁺**, **19aH₂²⁺**, and **19bH₂²⁺** in TFA–CDCl₃

molecule	22-H	9,18-H	8,19-H	13,14-H
11bH₂²⁺	5.29	7.22	7.97	7.98
19aH₂²⁺	3.65	7.23	7.97	7.86
19bH₂²⁺	4.69	7.15	7.97	8.00

in the case of **19aH₂²⁺** (Figure 6). As expected, **19bH₂²⁺** gave an intermediary value of 4.69 ppm. However, the downfield shifts for the pyrrolic protons showed virtually no changes apart from a slightly anomalous value of 7.15 ppm noted for the 9,18-H resonance in **19bH₂²⁺** (Table 3). For **19aH₂²⁺**, the thiophene protons were shifted approximately 0.2 ppm further downfield compared to **11bH₂²⁺** and **19bH₂²⁺**, but the effect is small. The modest effects resulting from the presence of the methoxy substituents are due to the strong steric interactions with the adjacent phenyl units which cause significant distortion to the macrocycle. In the carbon-13 NMR spectra for **19aH₂²⁺** and **19bH₂²⁺** in TFA–CDCl₃, the internal CH resonances were observed at 103.4 and 100.2 ppm, respectively. Again, both proton and carbon-13 NMR spectroscopy demonstrate that the dicationic species possess a plane of symmetry. The UV–vis spectrum for **19aH₂²⁺** in 1% TFA–chloroform gave rise to two broad Soret-like bands at 433 and 511 nm and a broad absorption at 851 nm (Figure 3). Similarly, the spectrum for **19bH₂²⁺** showed Soret-like bands at 424 and 489 nm and a broad absorption centered on 852 nm.

Palladium(II) Thiaoxybenzporphyrins. The metalation of dimethoxythiabenziporphyrins **19** was attempted using palladium(II) acetate, and it was anticipated that cationic complexes **20** could be generated (Scheme 6). When **19a** or **19b** was refluxed with Pd(OAc)₂ in acetonitrile, the reaction solution rapidly turned from green to a dark red color. After 5 min, TLC analysis showed that all of the starting porphyrinoid had been consumed. When the products of the reaction were purified on grade 3 basic alumina, two bands were collected. The first band (minor) eluted with dichloromethane, but a second polar band (major) was collected upon elution with 20% methanol–chloroform. Although the polar band may correspond in part to the anticipated products **20**, proton NMR spectroscopy showed the presence of complex mixtures that could not be further characterized. The proton NMR spectra for the nonpolar products showed that the macrocycles were no longer symmetrical (Figure 7) and demonstrated that one of the methoxy groups had been cleaved. In addition, the pyrrole and thiophene protons were substantially shifted downfield compared to the corresponding resonances in porphyrinoids **19** indicating that a fully aromatic species had been generated.

Scheme 6

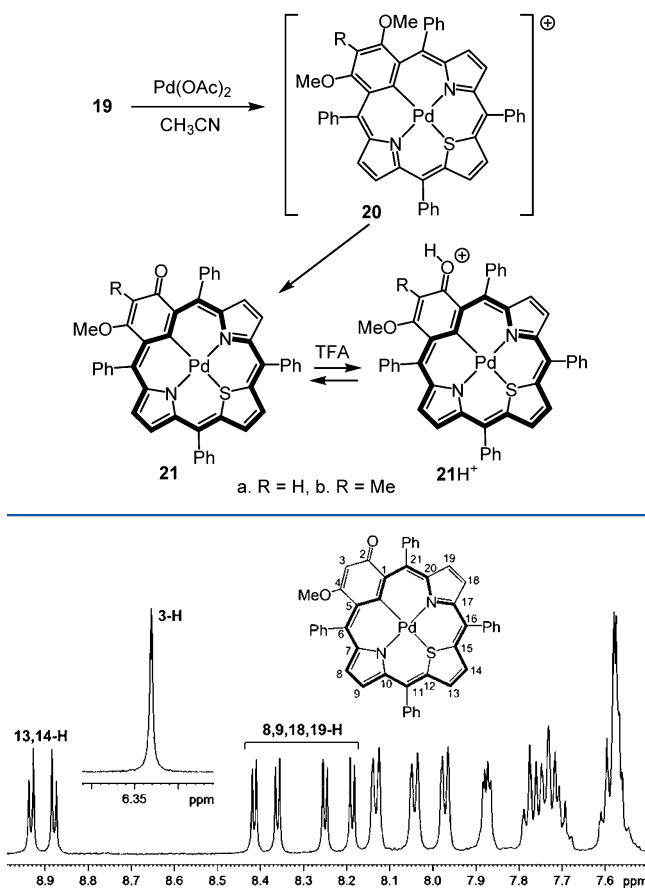
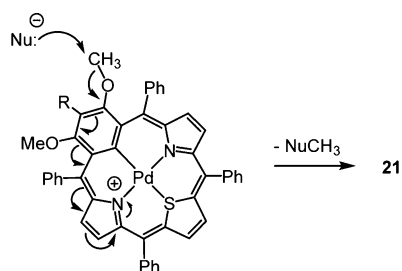
Palladium(II) thiaoxybenzporphyrins

Figure 7. Partial 500 MHz proton NMR spectrum of palladium(II) thiaoxybenzporphyrin **21a** in CDCl_3 showing details of the downfield region.

These results indicate that palladium complexes of methoxy-thiaoxybenzporphyrins **21** had been generated (Scheme 6). Initial yields of palladium complexes **21** were very low. The formation of these species is likely to involve a two-step process whereby initial insertion of palladium(II) affords **20**, followed by cleavage of a methoxy group to give **21**. In fact, the second step would involve a simple $\text{S}_{\text{N}}2$ -type reaction where a nucleophile displaces the palladium complexes **21** as leaving groups (Scheme 7). Under these reaction conditions, acetate may be the nucleophile that triggers this process. Using **19b**, when the reaction time was increased to 2 h (refluxing acetonitrile), the intermediary complex was no longer present,

Scheme 7



but the yield of **21b** was still only 11%. When the palladium source was changed to PdCl_2 , poorer results were obtained. After allowing the reaction to reflux for 16 h, residual **19** was still present along with the polar intermediate, but very little of the final product **21** had been formed. Chloride has a similar nucleophilicity to acetate ions,²⁶ and it is unclear why poorer results were obtained under these conditions. However, the basic acetate ion may be helping to deprotonate **19** and could thereby help to facilitate the initial metalation process. When the reaction was carried out with $\text{Pd}(\text{OAc})_2$ and potassium iodide, only minimal amounts of **21** were formed after 2 h. We had anticipated that the superior nucleophilicity of the iodide anion would enhance the formation of **21**, but instead the second step was inhibited. As the presence of a base may be a factor, the reaction of **19a** with $\text{Pd}(\text{OAc})_2$ was carried out in refluxing pyridine. The reaction did occur more rapidly in this case, and the polar intermediate was no longer present after 1 h. Following purification, **21a** was isolated in 18% yield. However, the best results were obtained when **19a** was refluxed with $\text{Pd}(\text{OAc})_2$ and sodium acetate in acetonitrile for 16 h, and the thiaoxybenzporphyrin complex **21a** was isolated in 34% yield. Under these conditions, **19b** reacted more rapidly and afforded **21b** in 60% yield following a 2 h reflux. The UV-vis spectrum for metalloporphyrinoid **21a** gave an absorption at 416 nm, a Soret-like band at 510 nm, and a broad absorption between 600 and 750 nm (Figure 8). In the presence of TFA, a new

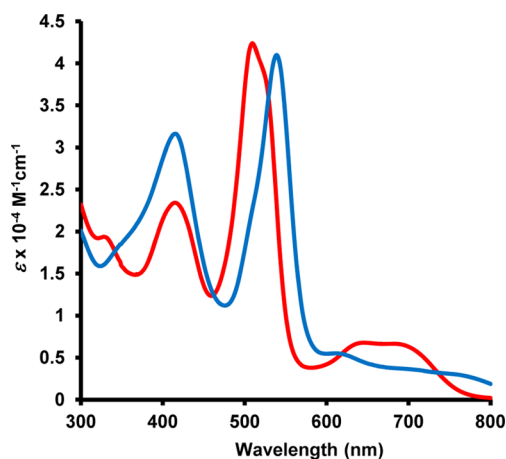


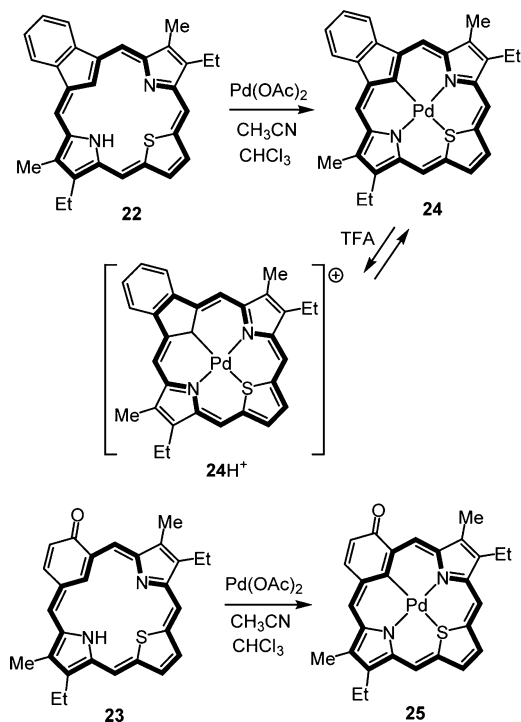
Figure 8. UV-vis spectra of palladium(II) methoxyoxybenzporphyrin **21a** in chloroform (red line) and 1% TFA-chloroform (cation **21aH**⁺, blue line).

chromophore was generated that showed a Soret-like band at 539 nm and a broader peak at 415 nm, and this was attributed to the formation of a cationic species **21aH**⁺. This process was reversible, and **21a** was regenerated upon addition of triethylamine. The 3-methyl-substituted complex **21b** gave similar results. The IR spectra for **21a** and **21b** gave carbonyl stretching frequencies at 1594 and 1628 cm^{-1} , respectively. The low value for **21a** is due in part to the electron-donating effects of the methoxy substituent, but this is less effective for **21b** due to the steric demands of the 3-methyl unit. The identities of the palladium(II) complexes were confirmed by high-resolution ESI mass spectrometry. Attempts were also made to react thiabenzporphyrins with nickel(II) acetate. As sulfur is a relatively large atom compared to nitrogen, it was anticipated that the smaller nickel(II) cation would fit more easily into the macrocyclic cavity. However, no metalation was observed in

these experiments, and unreacted starting material was recovered.

Thiacarba-porphyrinoids **22** and **23** had been prepared previously,²⁷ and the formation of palladium(II) derivatives for these compounds was also examined (Scheme 8). Refluxing

Scheme 8



22 and **23** with $\text{Pd}(\text{OAc})_2$ in acetonitrile rapidly afforded the corresponding palladium(II) complexes **24** and **25**, respectively, in good yields. These products were easily purified by column chromatography and recrystallized, but both derivatives were poorly soluble in organic solvents. Nevertheless, it was possible to obtain NMR data for these complexes. The proton NMR spectrum for palladium(II) benzothiacarba-porphyrin **24** in CDCl_3 was consistent with a fully aromatic porphyrinoid, and the *meso*-protons were observed as two 2H singlets at 10.04 and 10.46 ppm. The thiophene protons were also strongly shifted downfield to give a 2H singlet at 9.36 ppm. The proton and carbon-13 NMR spectra demonstrated that the complex retains a plane of symmetry. In the carbon-13 NMR spectrum, the *meso*-protons were identified at 110.7 and 111.0 ppm, while the external thiophene carbons gave a resonance at 129.9 ppm. The UV-vis spectrum for **24** gave two moderately strong bands at 403 and 501 nm and a broad absorption at 628 nm (Figure 9). Addition of TFA led to the formation of a new chromophore corresponding to a protonated species that showed a broad Soret band at 417 nm (Figure 9). The proton NMR spectrum of **24** in TFA- CDCl_3 produced two downfield 2H singlets at 10.07 and 10.24 ppm for the *meso*-protons, while the protons on the benzo-unit adjacent to the macrocycle ($2^1,3^1\text{-H}$) showed a pronounced downfield shift from 8.50 ppm in the free base to 9.07 ppm in the protonated form. This is consistent with the formation of a C-protonated species 24H^+ (Scheme 8) that relocates the 18π electron delocalization pathway through the benzo-unit. However, a resonance for the associated internal CH could not be located, and this assignment is considered to be tentative. Unfortunately, the sample was not sufficiently

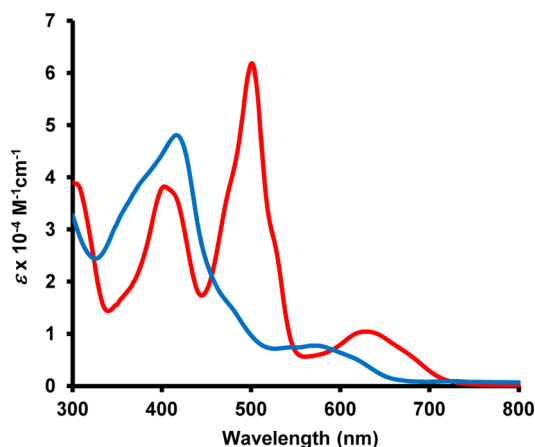


Figure 9. UV-vis spectrum of palladium(II) benzothiacarba-porphyrin **24** in chloroform (red line) and 5% TFA-chloroform (blue line).

stable under these conditions for a carbon-13 NMR spectrum to be obtained. However, the protonation is reversible, and the original complex **24** was regenerated on addition of triethylamine. Palladium(II) thiaoxybenzporphyrin **25** was poorly soluble, but NMR data could be obtained at 50 °C in CDCl_3 . This complex is also aromatic, and the proton NMR spectrum gave four 1H singlets for the *meso*-protons at 8.89, 9.63, 9.71, and 10.35 ppm. The carbon-13 NMR spectrum showed the presence of a carbonyl resonance at 188.8 ppm, while the IR spectrum of **25** gave a peak at 1627 cm^{-1} for the $\text{C}=\text{O}$ stretch. The UV-vis spectrum of **25** gave a strong Soret-like band at 507 nm and two weaker absorptions at 622 and 673 nm (Figure 10). Addition of TFA gave rise to a protonated species that

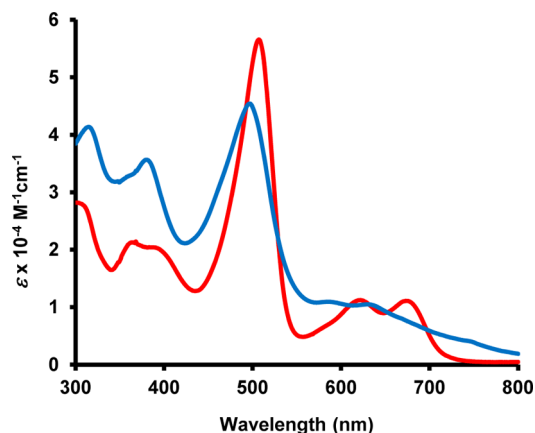


Figure 10. UV-vis spectrum of palladium(II) thiaoxybenzporphyrin **25** in chloroform (red line) and 1% TFA-chloroform (blue line).

showed a strong peak at 497 nm (Figure 10), but a proton NMR spectrum could not be obtained for this species in part because the complex slowly underwent demetalation. The identity of complexes **24** and **25** was supported by high-resolution ESI mass spectrometry.

Palladium complexes **21a**, **21b**, **24**, and **25** significantly expand the number of known metalated heterocarba-porphyrinoid derivatives. Previous examples include nickel, palladium, and platinum complexes of 23-oxabenzocarba-porphyrins **26**,²⁷ palladium(II) 22-oxabenzocarba-porphyrin **27**,²⁸ and palladium(II) oxa-oxybenzporphyrin **28**.²⁹ In a recent independent study, examples of palladium(II) complexes

of a thiacarboxyporphyrin (**29a**) and a thiachlorin (**29b**) have been described.³⁰ The metalated structures reported in the present study gave powders or microcrystalline materials that were not well suited for structural analysis. However, the X-ray structure of **21a** was obtained (Figure 11), and this established

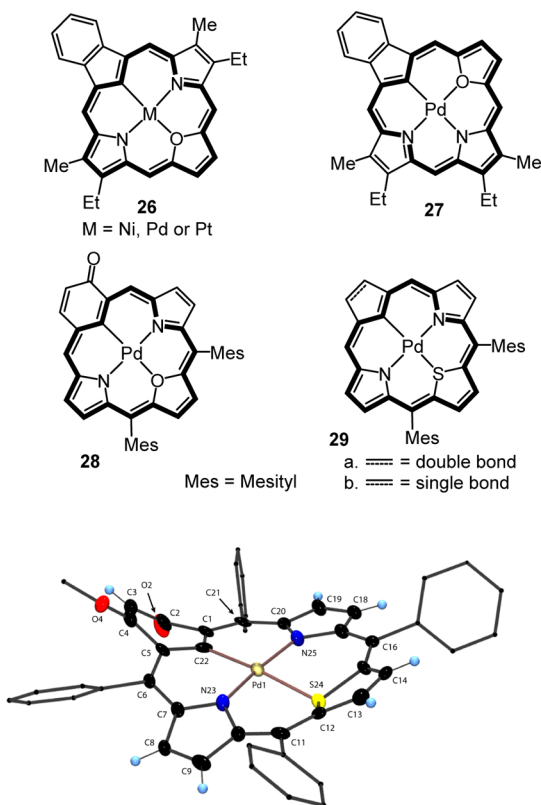


Figure 11. Color POV-Ray rendered ORTEP III drawing of compound **21a** (50% probability level, Ph and Me groups rendered as sticks for clarity, hydrogen atoms drawn arbitrarily small). Selected bond lengths (Å): Pd1–N25 2.029(6), Pd1–N23 2.036(6), Pd1–C22 2.037(8), Pd1–S24 2.250(2), C1–C2 1.528(11), C2–O2 1.253(9), C2–C3 1.413(11), C3–C4 1.340(10), C4–C5 1.477(11), C5–C22 1.423(10), C22–C1 1.387(10), C5–C6 1.397(10), C21–C1 1.419(10). Selected bond angles (deg): C22–Pd1–S24 172.3(2), N23–Pd1–N25 172.5(3), C22–Pd1–N23 94.0(3), C22–Pd1–N25 93.2(3), S24–Pd1–N23 87.4(2), S24–Pd1–N25 85.7(2).

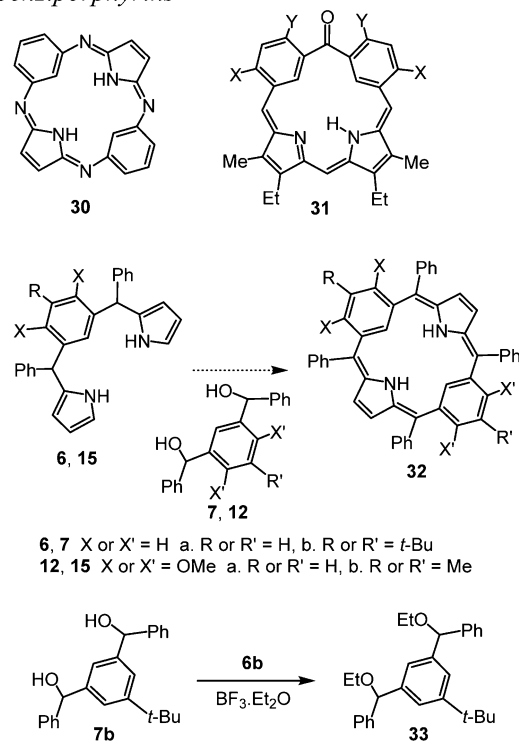
the presence of an organometallic Pd–C linkage and showed a uniquely distorted macrocyclic framework. Rather than the anticipated planar arrangement of sp^2 hybridized atoms, the oxybenzi moiety is distorted to a boat-like conformation. In fact, a Cremer–Pople³¹ ring-puckering analysis revealed a formally slightly twisted $C_{2v}^{C_5}$ boat conformation with $\theta = 92.2^\circ$ and $\phi = 229.2^\circ$. Particularly noteworthy are the exceptionally long $C_{(sp^2)}-C_{(sp^2)}$ bonds which appear to isolate the $MeO-CH=CH-C=O$ fragment from the rest of the macrocyclic framework's π -system. Specifically, C4–C5 is 1.477(11) Å while the C1–C2 separation is a remarkably long 1.528(11) Å. The overall structure exhibits framework bond distances consistent with a generally localized π -bonding model. As is typical, the phenyl substituents attached to the *meso*-carbon atoms exhibit π -systems separated from the main macrocycle. The metal coordination environment of **21a** is essentially the typical four-coordinate square-planar geometry characteristic of Pd(II) complexes; however, the large sulfur atom lies 0.310(2) Å away from the plane defined by Pd, C22,

N23, and N25. The 2.250(2) Å Pd–S distance in **21a**, however, appears to be reasonable when compared with the 2.32(6) Å distances observed for over 6500 crystallographically measured Pd–S bonds.³² The 2.037(8) Å Pd–C distance in **21a** is in close agreement with the 2.031(2) and 2.055(4) Å distances observed in the related palladium(II) benziporphyrin²⁰ and naphthiporphyrin⁹ complexes. This is consistent with the distances of 2.00(5) Å observed for nearly 3000 crystallographically measured complexes containing Pd–C(phenyl) σ bonds.³² The sulfur atom resides in a roughly trigonal pyramidal environment, being 0.657(2) Å away from the plane defined by C12, C15, and Pd. The observed angles between atoms connected to sulfur are 94.6(4)° for C15–S24–C12, 115.1(3)° for Pd–S24–C12, and 115.2(3)° for Pd–S24–C15.

Dibenziporphyrins. The successful synthesis of benziporphyrins and thiabenziporphyrins from dimethoxybenzotripyrranes encouraged us to consider the formation of new porphyrinoid systems by the same strategy. Although benziporphyrins are well studied, little is known about the properties of porphyrin analogues with two benzene subunits. Phthalocyanine analogues **30** with two benzene subunits have been known for over 60 years,^{33,34} and extensive studies on the metalation of this system have been conducted.^{35,36} Recently, we reported the synthesis of dibenzioxophlorins **31**, but these porphyrinoids proved to be somewhat unstable.³⁷ It was envisaged that analogues of **30** could be obtained by reacting a benzitripyrrane with a benzene dicarbinol such as **7** or **12** (Scheme 9). Four different benzitripyrranes, **6a,b** and **15a,b**, have been prepared, and four related benzene dicarbinols, **7a,b** and **12a,b**, were also available. In principle, these reactants might be combined to give 10 different dibenziporphyrin products **32**. Initial attempts to carry out this chemistry were

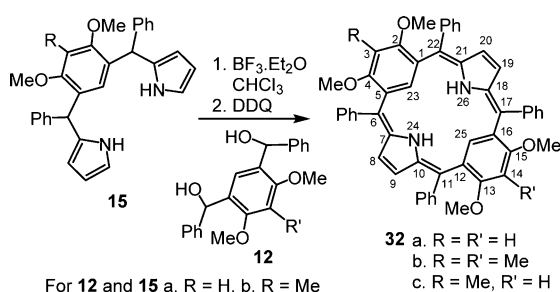
Scheme 9

Dibenziporphyrins



conducted using benzitripyrrane **6a** and dicarbinol **7a**. Reaction conditions were altered by varying the solvent, concentration, reaction time, and amount of acid catalyst used. In addition, an oxidation step was required, and these conditions were also investigated. Unfortunately, none of the reaction conditions considered produced any of the desired dibenziporphyrin. Attempts to react **6b** with **7b** were similarly unsuccessful. However, when these reactants were treated with boron trifluoride etherate in dichloromethane, a diether product **33** was generated as a mixture of diastereomers (Scheme 9). These problems were overcome when dimethoxybenzotripyrranes were utilized in these reactions. Tripyrrane analogue **15b** was condensed with dicarbinol **12b** in the presence of boron trifluoride etherate, and the mixture was subsequently oxidized with DDQ (Scheme 10). The product was initially purified on

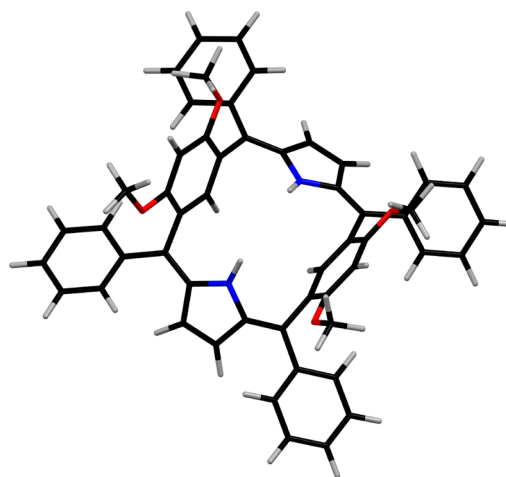
Scheme 10



an alumina column, and then on silica gel, and finally recrystallized from chloroform–hexanes. This approach gave the desired dibenziporphyrin **32b** in pure form, but inconsistent yields were obtained. The material obtained from the initial alumina column was very impure, but it was later found that recrystallization was all that was required to purify the material. When the silica column was avoided, dibenziporphyrin **32b** was isolated in a consistent 18% yield. The asymmetrical dibenziporphyrin **32c** might be obtained by two different routes using **12a** and **15b**, or **12b** and **15a** (Scheme 10). However, reaction of dicarbinol **12b** with benzitripyrrane **15a** gave dibenziporphyrin **32c** in only 5% yield, while the combination of **12a** and **15b** afforded a 13% yield. The oxidation time was crucial in these reactions. In the initial preparation of **32b**, the intermediate was exposed to DDQ for 10 min. However, in the preparation of **32c** this led to extensive decomposition, and it was necessary to reduce the oxidation time to no more than 5 min. Chloranil is a milder dehydrogenation agent, and attempts were made to use this in place of DDQ. However, these experiments did not produce any of the dibenziporphyrin product. Dibenziporphyrin **32a** was similarly obtained from the reaction of **12a** with **15a**. In this case, brief oxidation times were required. In addition, attempts to purify this product on a silica column led to extensive decomposition. Nevertheless, recrystallization from chloroform–methanol gave the pure product in 14% yield. Attempts to react dimethoxybenzene dicarbinols **12a,b** with benzitripyrranes **6a,b**, or dimethoxytripyrane analogues **15a,b** with **7a,b**, failed to give any dibenziporphyrin products. Therefore, only tetramethoxydibenziporphyrins could be prepared using this strategy.

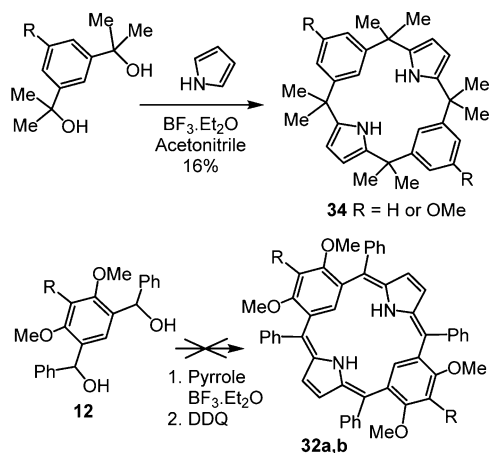
Tetramethoxydibenziporphyrins **32a–c** were isolated as orange powders. These macrocycles are not intensely colored like porphyrins and most porphyrin analogues because the system is doubly cross-conjugated. The UV–vis spectra for

32a–c gave a single strong absorption band near 420 nm. These compounds are very stable at room temperature as solids and can be stored in this form indefinitely, but gradual decomposition occurs in solution. This decomposition is associated with the orange-colored solutions turning red. Dibenziporphyrins **32b** and **32c** were sufficiently soluble in CDCl_3 to give NMR data, but the proton NMR spectrum for **32a** could only be obtained in deuterated benzene. As expected, this system did not show any macrocyclic aromatic properties. For instance, in the proton NMR spectrum of **32b** in CDCl_3 , the internal CH gave a resonance at 7.62 ppm. This is consistent with the presence of an isolated benzene unit. Attempts were made to synthesize metal complexes of **32a–c**. Reaction of **32b** with palladium(II) acetate in refluxing acetonitrile for 15 min did afford a product, albeit in low yield, but the proton NMR spectrum showed the presence of two compounds which could not be identified. Attempts to react **32** with nickel(II) acetate and silver(I) acetate were also unsuccessful. The inability of this system to afford metalated derivatives may be due in part to the anticipated nonplanarity of the macrocycle, as well as its instability at elevated temperatures. Unfortunately, it was not possible to obtain suitable crystals of **32a–c** for X-ray diffraction analysis, but the conformations of these porphyrinoids were assessed by computational methods. Geometry optimization was performed at the DFT level of theory with the B3LYP functional using a 6-311++G** basis set. The results showed that these structures are indeed very distorted and the individual subunits are rotated between 37.89° and 63.50° relative to the mean macrocyclic plane (Table 1 and Figure 12). NICS calculations were also performed on **32a–c**, and, as expected, the macrocycles showed negligible NICS(0) values of between -0.66 and -0.85 (see Supporting Information).

Figure 12. DFT-calculated conformation for dibenziporphyrin **32a**.

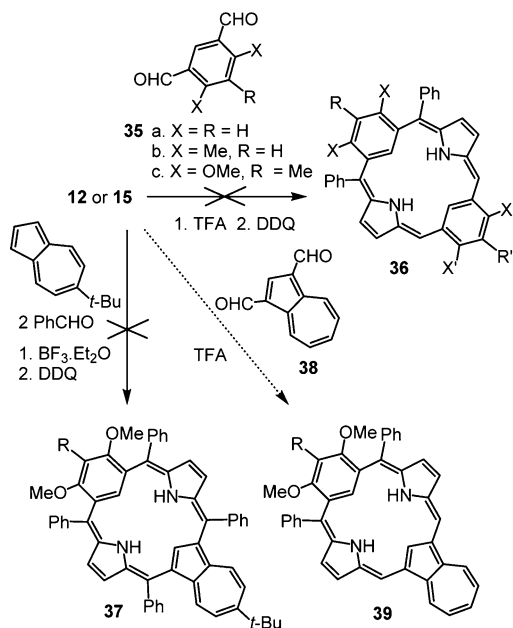
Symmetrical dibenziporphyrins **32a** and **32b** might potentially be synthesized using a one-pot method. A calix[2]-benzene[2]pyrrole **34** was previously prepared from a dicarbinol and pyrrole using this type of approach (Scheme 11),³⁸ and attempts were made to adapt this synthesis to the preparation of dibenziporphyrins, thereby eliminating the need for benzitripyrrane intermediates. Dicarbinols **12** were reacted with pyrrole in the presence of boron trifluoride etherate and subsequently oxidized with DDQ. However, no trace of the macrocyclic products could be identified (Scheme 11). The

Scheme 11



reaction of benzitripyrranes with isophthalaldehydes **35a–c** in the presence of TFA was also attempted, but this also failed to afford dibenziporphyrin products **36** (Scheme 12). The

Scheme 12



formation of porphyrin analogues with a benzene and an azulene subunit was also considered. Reaction of benzitripyrranes **15** with 6-*tert*-butylazulene and 2 equiv of benzaldehyde in the presence of boron trifluoride etherate, followed by oxidation with DDQ, failed to give the azulibenziporphyrin **37** (Scheme 12). However, reaction of azulene dialdehyde **38** with tripyrrane analogues **15** did show signs of macrocycle formation by proton NMR spectroscopy. Unfortunately, attempts to purify the crude products by column chromatography were unsuccessful, most likely due to the instability of the azulibenziporphyrin system.

CONCLUSIONS

Dimethoxybenzitripyrranes have proven to be versatile precursors in the synthesis of benziporphyrins and related macrocyclic systems. These tripyrrane analogues provide an alternative route to the synthesis of dimethoxybenziporphyrins

and have allowed the first syntheses of dimethoxythiabenziporphyrins. Both dimethoxybenzi- and thiabenziporphyrins exhibit a small degree of diatropic character that is enhanced upon protonation. In addition, dimethoxybenzi- and thiabenziporphyrins afforded stable organometallic derivatives when reacted with palladium(II) acetate. In the latter case, however, the metalation was accompanied by demethylation to afford aromatic palladium(II) thiaoxybenzporphyrins. Dimethoxybenzitripyrranes were also suitable precursors for the synthesis of the first examples of dibenziporphyrins. Although this system proved to be somewhat unstable, access to dibenziporphyrins highlights the versatility of this synthetic approach.

EXPERIMENTAL SECTION

Melting points are uncorrected. IR spectra were obtained on a FT-IR spectrometer equipped with an attenuated total reflectance (ATR) diamond cell. NMR spectra were recorded using a 400 or 500 MHz NMR spectrometer and were run at 300 K unless otherwise indicated. ^1H NMR values are reported as chemical shifts δ , relative integral, multiplicity (s, singlet; d, doublet; t, triplet; q, quartet; m, multiplet; br, broad peak), and coupling constant (*J*). Chemical shifts are reported in parts per million (ppm) relative to CDCl_3 (^1H residual CHCl_3 δ 7.26, ^{13}C CDCl_3 triplet δ 77.23) or C_6D_6 (^1H residual C_6HD_5 δ 7.15, ^{13}C C_6D_6 triplet δ 128.0), and coupling constants were taken directly from the spectra. NMR assignments were made with the aid of ^1H – ^1H COSY, HSQC, DEPT-135, and NOE difference proton NMR spectroscopy. 2D experiments were performed by using standard software. High-resolution mass spectra (HRMS) were obtained by using a double focusing magnetic sector instrument. ^1H and ^{13}C NMR spectra for all new compounds are reported in the Supporting Information. All calculations were performed using Gaussian 09, Revision D.01, running on a Linux-based PC. Energy minimization calculations of the benziporphyrinoid systems were performed at the Density Functional Theory (DFT) with the B3LYP functional and a 6-311++G(d,p) basis set. Mercury 3.1 running on an OS X platform, as provided by the CCDC, www.ccdc.cam.ac.uk/mercury/, was used to visualize the optimized structures. The resulting Cartesian coordinates of the molecules can be found in the Supporting Information section. NICS values were computed using the GIAO method, at the DFT level with the B3LYP functional and a 6-31+G(d,p) basis set, at several positions in each molecule. NICS(0) was calculated at the mean position of the four internal heavy atoms. NICS(a), NICS(b), NICS(c), and NICS(d) values were obtained by applying the same method to the center of each of the individual rings that make up the macrocycles.

4,6-Dimethoxy-1,3-bis(phenyl-2-pyrrolylmethyl)benzene (15a). Nitrogen was bubbled through a solution of dicarbinol **12a**¹⁵ (700 mg, 2.00 mmol) and freshly distilled pyrrole (20 mL, 0.29 mol) in 1,2-dichloroethane (40 mL) for 20 min, and then a 10% $\text{BF}_3 \cdot \text{Et}_2\text{O}$ solution in 1,2-dichloroethane (1.5 mL) was added. The solution was then refluxed under nitrogen for 17 h. The solution was allowed to cool to room temperature, triethylamine (2 mL) was added, and the mixture was allowed to stir for a few min. The solution was then concentrated under vacuum. The dark sticky residue was purified by column chromatography on silica, eluting with a mixture of hexanes, dichloromethane, and triethylamine in a 60:40:1 ratio. Residual pyrrole was eluted first, followed by the benzitripyrrane diastereomers. Column fractions containing the diastereomers were combined, and the solvent was evaporated under reduced pressure to yield the tripyrrane analogue (723 mg, 1.61 mmol, 81%) as a flaky off-white solid, mp 60–70 °C; ^1H NMR (500 MHz, CDCl_3) δ 3.72 (6H, s), 5.65, 5.66 (2H, 2 overlapping singlets), 5.73, 5.78 (2H, two triplets, *J* = 2.7 Hz), 6.05–6.08, 6.09–6.12 (2H, 2 multiplets), 6.46 (1H, s), 6.57–6.61, 6.61–6.65 (2H, two multiplets), 6.78, 6.81 (1H, two singlets), 7.02–7.25 (10H, m), 7.87–7.91 (2H, two overlapping singlets); ^{13}C NMR (125 MHz, CDCl_3) δ 43.6, 56.2, 56.2, 96.6, 96.7, 107.6, 107.7, 108.1, 108.2, 116.9, 124.16, 124.20, 126.29, 126.33, 128.29, 128.35, 128.6, 131.72,

131.74, 133.7, 133.9, 143.6, 143.9, 156.64, 156.66; HRMS (ESI⁺) calcd for C₃₀H₂₈N₂O₂ - H 447.2078, found 447.2085.

4,6-Dimethoxy-5-methyl-1,3-bis(phenyl-2-pyrrolylmethyl)-benzene (15b). Under the foregoing reaction conditions, **12b**¹⁵ (730.3 mg, 2.00 mmol) was reacted with freshly distilled pyrrole (20 mL, 0.29 mol) to produce **15b** (837 mg, 1.81 mmol, 90%) as a flaky off-white solid, mp 51–61 °C; ¹H NMR (500 MHz, CDCl₃) δ 2.23 (3H, s), 3.41 (6H, 2 overlapping singlets), 5.68, 5.69 (2H, 2 overlapping singlets), 5.72–5.75 (1H, m), 5.79–5.83 (1H, m), 6.08 (1H, q, *J* = 2.9 Hz), 6.12 (1H, q, *J* = 2.9 Hz), 6.60–6.63 (1H, m), 6.65–6.68 (1H, m), 7.05 (2H, d, *J* = 7.5 Hz), 7.10 (2H, d, *J* = 7.5 Hz), 7.14–7.32 (7H, m), 8.00 (1H, s), 8.08 (1H, s); ¹³C NMR (125 MHz, CDCl₃) δ 10.5, 44.47, 44.50, 60.8, 107.9, 108.0, 108.2, 108.3, 117.2, 124.84, 124.89, 126.52, 126.58, 128.44, 128.51, 128.69, 128.72, 129.4, 129.5, 132.41, 132.43, 133.4, 133.7, 143.7, 144.0, 156.01, 156.07; HRMS (ESI⁺) calcd for C₃₁H₃₀N₂O₂ - H 461.2235, found 461.2229.

13,14-Diethyl-2,4-dimethoxy-6,21-diphenylbenzoporphyrin (16a). Nitrogen was bubbled through a solution of benzitripyrrane **15a** (50 mg, 0.11 mmol) and pyrrole dialdehyde **8**^{39,40} (20 mg, 0.11 mmol) in chloroform (50 mL) for 10 min. TFA (0.5 mL) was added and the solution stirred, protected from light, for 2 h under nitrogen. DDQ (26 mg, 0.11 mmol) was added and the solution stirred for a further 1 h. The reaction mixture was washed with water, saturated sodium bicarbonate solution (×2), and water and then concentrated. The residue was chromatographed on grade 3 neutral alumina, eluting with dichloromethane. A blue band eluted off first which corresponded to phlorin **17a**, followed by a dark green band which was collected, and solvent was removed under reduced pressure to yield **16a** (27 mg, 0.046 mmol, 42%) as a dark green powder, mp >300 °C; UV-vis (1% Et₃N-CHCl₃) λ_{max} (log ε) 320 (3.97), 421 (4.56), 616 (sh, 3.97), 659 nm (4.00); UV-vis (1% TFA-CHCl₃) λ_{max} (log ε) 430 (4.79), 564 (3.75), 611 (3.78), 689 (sh, 3.89), 765 nm (4.22); ¹H NMR (500 MHz, CDCl₃) δ 1.25 (6H, t, *J* = 7.6 Hz, 2×CH₂CH₃), 2.69 (4H, q, *J* = 7.6 Hz, 13,14-CH₂), 3.33 (6H, s, 2×OCH₃), 5.93 (1H, br s, 22-H), 6.27 (2H, s, 11,16-H), 6.36 (1H, s, 3-H), 6.97 (2H, d, *J* = 4.6 Hz, 9,18-H), 7.36–7.39 (2H, m, *p*-Ph), 7.41–7.44 (4H, m, *m*-Ph), 7.50 (2H, d, *J* = 4.6 Hz, 8,19-H), 7.55–7.58 (4H, m, *o*-Ph), 9.19 (1H, br s, NH); ¹H NMR (500 MHz, TFA-CDCl₃, dication **16aH₂²⁺**) δ 1.36 (6H, t, *J* = 7.7 Hz, 2×CH₂CH₃), 2.90–3.03 (4H, m, 13,14-CH₂), 3.45 (6H, s, 2×OCH₃), 3.77 (1H, s, 22-H), 5.37 (1H, br s, 24-NH), 6.52 (1H, s, 3-H), 7.27 (2H, s, 11,16-H), 7.56 (2H, dd, *J* = 1.4, 5.0 Hz, 9,18-H), 7.64–7.68 (4H, m, *m*-Ph), 7.69–7.73 (2H, m, *p*-Ph), 7.76–7.79 (4H, m, *o*-Ph), 7.95 (2H, dd, *J* = 1.5, 5.0 Hz, 8,19-H), 8.55 (2H, s, 23,25-NH); ¹³C NMR (125 MHz, CDCl₃) δ 15.9 (2×CH₂CH₃), 17.9 (13,14-CH₂), 55.6 (2×OCH₃), 95.5 (11,16-CH), 98.5 (3-CH), 110.4 (22-CH), 122.1, 127.3 (*m*-Ph), 127.5 (*p*-Ph), 130.7 (9,18-CH), 131.4 (*o*-Ph), 136.0 (8,19-CH), 139.9, 140.8, 143.6, 148.0, 156.5, 159.3, 168.6; ¹³C NMR (125 MHz, TFA-CDCl₃, dication **16aH₂²⁺**) δ 15.3 (2×CH₂CH₃), 18.5 (13,14-CH₂), 56.4 (2×OCH₃), 95.6 (11,16-CH), 99.9 (3-CH), 101.2 (22-CH), 122.0, 127.8 (9,18-CH), 129.0 (*m*-Ph), 132.1 (*p*-Ph), 133.1 (*o*-Ph), 138.0 (8,19-CH), 139.8, 143.9, 145.6, 147.2, 151.4, 157.9, 163.8; HRMS (ESI⁺) calcd for C₄₀H₃₃N₃O₂ + H 590.2808, found 590.2806.

13,14-Diethyl-2,4-dimethoxy-3-methyl-6,21-diphenylbenzoporphyrin (16b). Nitrogen was bubbled through a solution of benzitripyrrane **15b** (25.5 mg, 0.055 mmol) and pyrrole dialdehyde **8**^{39,40} (10 mg, 0.056 mmol) in chloroform (30 mL) for 5 min. TFA (250 μL) was added via syringe, and the solution turned dark red. The solution was stirred under nitrogen protected from light for 2 h. DDQ (13 mg, 0.057 mmol) was added, and the mixture was stirred for a further 1 h. The dark brown solution was washed with 5% sodium bicarbonate (turning the solution dark green) and water, back extracting each time with chloroform. The organic phases were combined, and the solvent was evaporated under reduced pressure. The residue was purified by column chromatography on grade 3 neutral alumina, eluting with dichloromethane. The first blue band to elute off the column corresponded to phlorin **17b**, while the second dark green band corresponded to the benzoporphyrin. The dark green band was collected, and the solvent was evaporated under reduced pressure to afford **16b** (23 mg, 0.038 mmol, 69%) as a dark green

solid, mp >300 °C; UV-vis (1% Et₃N-CHCl₃) λ_{max} (log ε) 409 (4.73), 656 (4.04); UV-vis (1% TFA-CHCl₃) λ_{max} (log ε) 442 (4.85), 774 (4.21); ¹H NMR (500 MHz, CDCl₃) δ 1.22 (6H, t, *J* = 7.7 Hz, 2×CH₂CH₃), 1.98 (3H, s, 3-CH₃), 2.55–2.69 (4H, m, 13,14-CH₂), 3.23 (6H, s, 2×OCH₃), 6.10 (2H, s, 11,16-H), 6.42 (1H, s, 22-H), 6.91 (2H, d, *J* = 4.6 Hz, 9,18-H), 7.40–7.47 (6H, m, *m*- and *p*-Ph), 7.51 (2H, d, *J* = 4.6 Hz, 8,19-H), 7.54–7.56 (4H, m, *o*-Ph), 9.82 (1H, br s, NH); ¹H NMR (500 MHz, TFA-CDCl₃, dication **16bH₂²⁺**) δ 1.28 (6H, t, *J* = 7.6 Hz, 2×CH₂CH₃), 2.01 (3H, s, 3-CH₃), 2.74–2.88 (4H, m, 13,14-CH₂), 3.17 (6H, s, 2×OCH₃), 5.07 (1H, s, 22-H), 6.90 (2H, s, 11,16-H), 7.01 (1H, br s, 24-NH), 7.41 (2H, d, *J* = 5.0 Hz, 9,18-H), 7.64–7.74 (10H, m, 2×Ph), 7.91 (2H, d, *J* = 5.0 Hz, 8,19-H), 10.10 (2H, br s, 23,25-NH); ¹³C NMR (125 MHz, CDCl₃) δ 10.2 (3-CH₃), 15.7 (2×CH₂CH₃), 17.8 (13,14-CH₂), 61.1 (2×OCH₃), 95.6 (11,16-H), 108.4 (22-H), 126.9, 127.7 (*m*-Ph), 128.2 (*p*-Ph), 129.5, 131.1 (*o*-Ph), 131.3 (9,18-CH), 135.9 (8,19-CH), 140.1, 141.2, 142.6, 148.6, 157.1, 157.3, 169.4; ¹³C NMR (125 MHz, TFA-CDCl₃, dication **16bH₂²⁺**) δ 11.0 (3-CH₃), 15.1 (2×CH₂CH₃), 18.3 (13,14-CH₂), 62.5 (2×OCH₃), 95.9 (11,16-CH), 97.5 (22-CH), 128.6, 128.8 (9,18-CH), 129.3 (*m*-Ph), 130.6, 132.5, 132.6 (*o*,*p*-Ph), 138.8 (8,19-CH), 139.5, 144.3, 146.0, 148.3, 153.1, 160.4, 162.1; HR MS (ESI⁺) calcd for C₄₁H₃₇N₃O₂ + H 604.2964, found 604.2966.

13,14-Diethyl-2,4-dimethoxy-3-methyl-6,21-diphenyl-6,25-dihydro-23H-benzoporphyrin (17b). The solvent was evaporated from the blue fraction (see above) under reduced pressure and the residue further purified by recrystallization from chloroform-methanol to give the phlorin (3.5 mg, 0.0058 mmol, 10%) as a dark powder, mp 246–249 °C; UV-vis (1% Et₃N-CHCl₃) λ_{max} (log ε) 381 (4.63), 587 (sh, 4.27), 623 nm (4.32); UV-vis (1% TFA-CHCl₃) λ_{max} (log ε) 411 (4.54), 514 (4.07), 672 (sh, 3.94), 734 nm (4.22); ¹H NMR (500 MHz, CDCl₃) δ 1.09 (3H, t, *J* = 7.5 Hz), 1.13 (3H, t, *J* = 7.5 Hz), 2.06 (3H, s), 2.42–2.52 (2H, m), 2.53–2.60 (2H, m), 3.16 (3H, s), 3.59 (3H, s), 5.77 (1H, s), 6.04 (1H, s), 6.41 (1H, s), 6.46 (1H, d, *J* = 3.5 Hz), 6.71 (1H, d, *J* = 3.5 Hz), 6.72 (1H, s), 6.74 (1H, d, *J* = 5.4 Hz), 6.90 (2H, d, *J* = 7.5 Hz), 7.03–7.06 (2H, m), 7.10 (2H, t, *J* = 7.5 Hz), 7.17–7.20 (4H, m), 7.25 (2H, t, *J* = 7.4 Hz), 7.84 (1H, v br), 9.57 (1H, br s); ¹³C NMR (125 MHz, CDCl₃) δ 10.0, 15.9, 17.1, 18.15, 18.17, 43.5, 60.4, 62.4, 91.1, 111.5, 112.5, 118.24, 118.27, 118.7, 125.6, 126.5, 127.0, 128.0, 128.5, 128.6, 128.7, 128.9, 129.8, 130.0, 132.2, 133.0, 138.7, 139.2, 141.4, 142.64, 142.68, 145.9, 148.8, 150.3, 156.2, 157.5, 166.2; HRMS (ESI⁺) calcd for C₄₁H₃₉N₃O₂ + H 606.3121, found 606.3129.

[13,14-Diethyl-2,4-dimethoxy-6,21-diphenylbenzoporphyrinato]palladium(II) (18a). Dimethoxybenzoporphyrin **16a** (9.5 mg, 0.016 mmol) and palladium(II) acetate (9.5 mg, 0.042 mmol) in acetonitrile (10 mL) were refluxed for 30 min. The solution was allowed to cool to room temperature and then diluted to 25 mL with dichloromethane. The solution was washed with water and back extracted with dichloromethane, the organic layers were combined, and the solvent was evaporated under reduced pressure. The residue was purified by column chromatography on grade 3 basic alumina, eluting with dichloromethane. A reddish-brown fraction was collected, the solvent evaporated under reduced pressure, and the residue recrystallized from chloroform-methanol to give the palladium complex (6.4 mg, 0.0092 mmol, 58%) as purple needles, mp 292–294 °C; UV-vis (CHCl₃) λ_{max} (log ε) 448 (4.71), 544 (3.93), 584 (4.24), 637 (3.53), 698 (3.74), 766 nm (3.87); ¹H NMR (500 MHz, CDCl₃) δ 1.47 (6H, t, *J* = 7.6 Hz, 2×CH₂CH₃), 3.12 (4H, q, *J* = 7.6 Hz, 13,14-CH₂), 3.31 (6H, s, 2×OCH₃), 6.18 (1H, s, 3-H), 7.38 (2H, t, *J* = 7.3 Hz, *p*-Ph), 7.46 (4H, t, *J* = 7.5 Hz, *m*-Ph), 7.65–7.68 (6H, m, *o*-Ph and 9,18-H), 7.73 (2H, s, 11,16-H), 7.84 (2H, d, *J* = 5.0 Hz, 8,19-H); ¹³C NMR (125 MHz, CDCl₃) δ 16.9 (2×CH₂CH₃), 18.8 (13,14-CH₂), 55.8 (2×OCH₃), 95.4 (3-CH), 98.7 (11,16-CH), 123.1, 126.1 (*p*-Ph), 126.7 (*m*-Ph), 129.0 (9,18-CH), 131.5 (*o*-Ph), 134.7 (8,19-CH), 138.4, 143.3, 144.9, 145.7, 150.88, 150.90, 154.6, 170.6; HRMS (ESI⁺) calcd for C₄₀H₃₃N₃O₂Pd + H 694.1686, found 694.1685.

[13,14-Diethyl-2,4-dimethoxy-3-methyl-6,21-diphenylbenzoporphyrinato]palladium(II) (18b). Under the foregoing reaction conditions, dimethoxybenzoporphyrin **16b** (10.1 mg, 0.017 mmol) and palladium(II) acetate (10.0 mg, 0.045 mmol) were reacted together to

produce the palladium complex (7.9 mg, 0.011 mmol, 65%) as a dark purple powder, 250–252 °C dec; UV-vis (CHCl_3) λ_{max} (log ϵ) 440 (4.60), 543 (3.90), 580 (3.96), 746 (3.60), 808 nm (3.60); ^1H NMR (500 MHz, CDCl_3) δ 1.39 (6H, t, J = 7.6 Hz, $2\times\text{CH}_2\text{CH}_3$), 1.91 (3H, s, 3- CH_3), 2.96 (4H, q, J = 7.6 Hz, 13,14- CH_2), 3.19 (6H, s, $2\times\text{OCH}_3$), 7.30 (2H, s, 11,16-H), 7.38–7.42 (4H, m, 9,18-H and p -Ph), 7.47 (4H, t, J = 7.4 Hz, m -Ph), 7.60 (4H, d, J = 7.4 Hz, o -Ph), 7.69 (2H, d, J = 5.0 Hz, 8,19-H); ^{13}C NMR (125 MHz, CDCl_3) δ 11.0 (3- CH_3), 16.6 ($2\times\text{CH}_2\text{CH}_3$), 18.5 (13,14- CH_2), 63.0 ($2\times\text{OCH}_3$), 98.8 (11,16-CH), 121.2, 126.8 (p -Ph), 127.0 (m -Ph), 128.7, 129.7 (9,18-CH), 131.0 (o -Ph), 135.2 (8,19-CH), 139.8, 143.6, 144.5, 146.7, 149.6, 152.7, 157.2, 168.2; HRMS (ESI^+) calcd for $\text{C}_{41}\text{H}_{35}\text{N}_3\text{O}_2\text{Pd} + \text{H}$ 708.1842, found 708.1845.

2,4-Dimethoxy-6,11,16,21-tetraphenyl-24-thiabenziporphyrin (19a). Nitrogen was bubbled through a solution of dimethoxybenzotripyrrane **15a** (131 mg, 0.290 mmol) and thiophene dicarbinol **10b**²⁴ (86.5 mg, 0.29 mmol) in chloroform (90 mL) for 10 min. A 10% $\text{BF}_3\cdot\text{Et}_2\text{O}$ solution in chloroform (200 μL) was added, and the solution was allowed to stir under nitrogen protected from light at room temperature for 2 h. DDQ (194 mg, 0.855 mmol) was added, and stirring was continued for a further 10 min. The solution was washed with water and concentrated under reduced pressure. The residue was purified by column chromatography on grade 3 neutral alumina, eluting with dichloromethane. A dark green band was collected, and the solvent was evaporated under reduced pressure to afford **19a** (81 mg, 0.12 mmol, 41%) as a dark green powder, mp >300 °C; UV-vis (1% $\text{Et}_3\text{N}-\text{CHCl}_3$) λ_{max} (log ϵ) 346 (4.47), 437 (4.45), 637 nm (4.06); UV-vis (1% TFA- CHCl_3) λ_{max} (log ϵ) 338 (4.29), 433 (4.58), 511 (4.57), 699 (3.91), 851 nm (4.17); ^1H NMR (125 MHz, CDCl_3) δ 3.41 (6H, s, $2\times\text{OCH}_3$), 6.34 (1H, br s, 22-H), 6.42 (1H, s, 3-H), 6.58 (2H, d, J = 4.6 Hz), 7.19 (2H, s, 13,14-H), 7.37–7.46 (18H, m), 7.56 (4H, d, 7.5 Hz); ^1H NMR (500 MHz, TFA- CDCl_3) δ 3.51 (6H, s, $2\times\text{OCH}_3$), 3.65 (1H, s, 22-H), 6.57 (1H, s, 3-H), 7.24 (2H, d, J = 4.9 Hz, 9,18-H), 7.67–7.74 (14H, m), 7.79–7.84 (6H, m), 7.95 (2H, d, J = 4.9 Hz, 8,19-H), 8.20 (2H, s, 13,14-H), 9.53 (2H, br s, $2\times\text{NH}$); ^{13}C NMR (125 MHz, CDCl_3) δ 55.6, 97.9, 122.9, 127.6, 127.8, 128.27, 128.33, 129.75, 129.76, 131.3, 131.4, 135.3, 135.9, 139.1, 143.0, 145.5, 154.3, 155.4, 159.7, 163.2, 170.7; ^{13}C NMR (125 MHz, TFA- CDCl_3) δ 56.7 ($2\times\text{OCH}_3$), 99.3 (3-CH), 103.4 (22-CH), 122.7, 128.2 (9,18-CH), 128.3, 129.5, 129.7, 131.3, 133.0, 133.6, 133.9, 135.8, 138.2 (8,19-CH), 139.8, 141.1 (13,14-CH), 143.4, 152.2, 153.3, 161.5, 165.1; HRMS (EI) calcd for $\text{C}_{48}\text{H}_{34}\text{N}_2\text{O}_2\text{S}$ 702.2341, found 702.2365.

2,4-Dimethoxy-3-methyl-6,11,16,21-tetraphenyl-24-thiabenziporphyrin (19b). Under the foregoing reaction conditions, **15b** (135.4 mg, 0.29 mmol) was reacted with thiophene dicarbinol **10b**²⁴ (87.2 mg, 0.29 mmol) to produce the thiabenziporphyrin (77 mg, 0.11 mmol, 38%) as a dark green powder, mp >300 °C; UV-vis (1% $\text{Et}_3\text{N}-\text{CHCl}_3$) λ_{max} (log ϵ) 347 (4.45), 421 (4.58), 632 nm (4.09); UV-vis (1% TFA- CHCl_3) λ_{max} (log ϵ) 339 (4.34), 424 (4.58), 489 (4.74), 685 (sh, 3.94), 852 nm (4.19); ^1H NMR (500 MHz, CDCl_3) δ 2.06 (3H, s, 3- CH_3), 3.31 (6H, s, $2\times\text{OCH}_3$), 6.56 (2H, d, J = 4.7 Hz), 6.67 (1H, s, 22-H), 7.11 (2H, s, 13,14-H), 7.38–7.49 (18H, m), 7.55 (4H, d, J = 7.6 Hz); ^1H NMR (500 MHz, TFA- CDCl_3) δ 2.05 (3H, s, 3- CH_3), 3.22 (6H, s, $2\times\text{OCH}_3$), 4.69 (1H, s, 22-H), 7.15 (2H, d, J = 5.0 Hz, 9,18-H), 7.59–7.69 (10H, m), 7.71–7.78 (8H, m), 7.82 (2H, t, J = 7.1 Hz), 7.97 (2H, d, J = 5.0 Hz, 8,19-H), 8.00 (2H, s, 13,14-H), 10.79 (2H, br s, $2\times\text{NH}$); ^{13}C NMR (125 MHz, CDCl_3) δ 10.5 (3- CH_3), 61.0 ($2\times\text{OCH}_3$), 113.9 (22-H), 126.3, 127.9, 128.0, 128.4, 128.9, 129.8, 130.28, 130.34, 131.1, 131.2, 135.5 (13,14-CH), 135.9, 138.9, 142.2, 145.6, 154.6, 155.8, 158.0, 171.3; ^{13}C NMR (125 MHz, TFA- CDCl_3) δ 11.7 (3- CH_3), 62.7 ($2\times\text{OCH}_3$), 100.2 (22-CH), 128.51, 128.53, 129.1 (9,18-CH), 129.4, 129.74, 129.76, 131.6, 132.5, 133.3, 134.1, 135.3, 139.3 (8,19-CH), 139.7, 141.6 (13,14-CH), 143.7, 153.7, 154.1, 163.3, 164.0; HRMS (EI) calcd for $\text{C}_{49}\text{H}_{36}\text{N}_2\text{O}_2\text{S}$ 716.2498, found 716.2498.

[4-Methoxy-6,11,16,21-tetraphenyl-24-thiaoxybenzporphyrinato]palladium(II) (21a). Dimethoxythiabenziporphyrin **19a** (9.6 mg, 0.014 mmol), palladium(II) acetate (10.5 mg, 0.047 mmol), and sodium acetate (10.5 mg, 0.128 mmol) in acetonitrile (10

mL) were stirred under reflux for 16 h. The solution was allowed to cool to room temperature, diluted to 25 mL with dichloromethane, washed with water, and back extracted with dichloromethane. The combined organic layers were dried over sodium sulfate and concentrated under reduced pressure. The residue was chromatographed on grade 3 basic alumina, eluting with dichloromethane. A red band was collected and evaporated to dryness under reduced pressure to give the palladium complex (3.8 mg, 0.0048 mmol, 34%) as a dark red solid, mp >300 °C; IR: $\nu_{\text{C=O}}$ 1594 cm^{-1} ; UV-vis (CHCl_3) λ_{max} (log ϵ) 329 (4.27), 416 (4.37), 510 (4.63), 524 (sh, 4.59), 648 nm (3.82); UV-vis (1% TFA- CHCl_3) λ_{max} (log ϵ) 415 (4.50), 539 nm (4.61); ^1H NMR (500 MHz, CDCl_3) δ 3.33 (3H, s, OCH_3), 6.33 (1H, s, 3-H), 7.54–7.61 (6H, m), 7.68–7.80 (6H, m), 7.86–7.89 (2H, m), 7.97 (2H, d, J = 7.2 Hz), 8.04 (2H, d, J = 7.2 Hz), 8.13 (2H, d, J = 7.4 Hz), 8.19 (1H, d, J = 4.8 Hz), 8.25 (1H, d, J = 4.8 Hz), 8.36 (1H, d, J = 4.8 Hz), 8.41 (1H, d, J = 4.8 Hz), 8.89 (1H, d, J = 5.1 Hz), 8.93 (1H, d, J = 5.1 Hz); ^{13}C NMR (125 MHz, CDCl_3) δ 55.4 (OCH_3), 102.4 (3-CH), 122.4, 126.48, 126.52, 126.7, 127.04, 127.05, 127.12, 128.4, 128.8, 129.0, 129.1, 130.4, 130.5, 131.5, 132.3, 132.5, 132.7, 133.0, 134.0, 134.1, 134.4, 134.71, 134.73, 136.4, 137.4, 140.5, 140.9, 141.2, 141.5, 142.5, 144.0, 145.54, 145.56, 149.2, 149.7, 149.8, 175.4, 195.3 (C=O); HRMS (ESI^+) calcd for $\text{C}_{47}\text{H}_{30}\text{N}_2\text{O}_2\text{PdS} + \text{H}$ 793.1141, found 793.1137.

[4-Methoxy-3-methyl-6,11,16,21-tetraphenyl-24-thiaoxybenzporphyrinato]palladium(II) (21b). Dimethoxythiabenziporphyrin **19b** (14.5 mg, 0.020 mmol), palladium(II) acetate (14.5 mg, 0.066 mmol), and sodium acetate (14.5 mg, 0.177 mmol) in acetonitrile (14.5 mL) were refluxed for 2 h. The product was purified as described for the previous procedure to give the palladium complex (8.2 mg, 0.012 mmol, 60%) as a dark solid, mp >300 °C; IR: $\nu_{\text{C=O}}$ 1628 cm^{-1} ; UV-vis (CHCl_3) λ_{max} (log ϵ) 415 (4.42), 514 (4.65), 530 (sh, 4.61), 645 (sh, 3.83), 705 nm (3.88); UV-vis (2% TFA- CHCl_3) λ_{max} (log ϵ) 421 (4.59), 543 nm (4.49); ^1H NMR (500 MHz, CDCl_3) δ 2.20 (3H, s, 3- CH_3), 2.97 (3H, s, OCH_3), 7.55–7.65 (6H, m), 7.68–7.81 (6H, m), 7.82–7.85 (2H, m), 8.03–8.07 (4H, m), 8.15–8.17 (2H, d, 7.2 Hz), 8.210 (1H, d, J = 4.8 Hz), 8.213 (1H, d, J = 4.8 Hz), 8.36 (1H, d, J = 4.8 Hz), 8.41 (1H, d, J = 4.8 Hz), 8.86 (1H, d, J = 5.2 Hz), 8.92 (1H, d, J = 5.2 Hz); ^{13}C NMR (125 MHz, CDCl_3) δ 9.4 (3- CH_3), 58.8 (OCH_3), 121.3, 121.6, 126.68, 126.73, 126.9, 127.0, 127.8, 128.4, 128.8, 129.1, 130.4, 130.6, 132.0, 132.38, 132.40, 132.9, 133.98, 134.05, 134.48, 134.55, 134.7, 136.4, 137.4, 139.6, 140.3, 141.1, 141.5, 142.1, 144.4, 144.5, 145.4, 148.8, 149.7, 149.9, 169.7, 197.9 (C=O); HRMS (ESI^+) calcd for $\text{C}_{48}\text{H}_{32}\text{N}_2\text{O}_2\text{PdS} + \text{H}$ 807.1298, found 807.1302.

[8,17-Diethyl-7,18-dimethyl-23-thia-benzo[b]carba-porphyrinato]palladium(II) (24). A mixture of benzothiacarba-porphyrin **22**²⁷ (10.0 mg, 0.019 mmol) and palladium(II) acetate (10.0 mg, 0.044 mmol) in acetonitrile (10 mL) and chloroform (10 mL) was stirred under reflux for 10 min. The mixture was washed with water and back extracted with chloroform, and the solvent was removed under reduced pressure. The residue was purified on a grade 3 alumina column, eluting with dichloromethane. Recrystallization from chloroform–methanol gave the palladium complex (11.1 mg, 0.018 mmol, 92%) as dark microcrystals, mp >300 °C; UV-vis (CHCl_3) λ_{max} (log ϵ) 403 (4.58), 501 (4.79), 628 nm (4.02); UV-vis (5% TFA- CHCl_3) λ_{max} (log ϵ) 417 (4.68), 572 nm (3.89); ^1H NMR (500 MHz, CDCl_3) δ 1.80 (6H, t, J = 7.7 Hz, $2\times\text{CH}_2\text{CH}_3$), 3.48 (6H, s, 7,18- CH_3), 3.88 (4H, q, J = 7.7 Hz, 8,17- CH_2), 7.49–7.52 (2H, m, $2^2,3^2$ -H), 8.48–8.51 (2H, m, $2^1,3^1$ -H), 9.36 (2H, s, 12,13-H), 10.04 (2H, s, 5,20-H), 10.46 (2H, s, 10,15-H); ^{13}C NMR (500 MHz, TFA- CDCl_3) δ 1.69 (6H, t, J = 7.7 Hz, $2\times\text{CH}_2\text{CH}_3$), 3.25 (6H, s, 7,18- CH_3), 3.55–3.69 (4H, m, 8,17- CH_2), 8.24–8.27 (2H, m, $2^2,3^2$ -H), 9.02 (2H, s, 13,14-H), 9.06–9.09 (2H, m, $2^1,3^1$ -H), 10.07 (2H, s), 10.24 (2H, s) ($4\times\text{meso-H}$); ^{13}C NMR (125 MHz, CDCl_3) δ 11.9 (7,18- CH_3), 17.6 ($2\times\text{CH}_2\text{CH}_3$), 20.3 (8,17- CH_2), 110.7 (5,20-CH), 111.0 (10,15-CH), 119.7 ($2^2,3^2$ -CH), 127.0 ($2^1,3^1$ -CH), 129.9 (12,13-CH), 134.1, 139.7, 142.8, 143.2, 145.5, 146.6; HRMS (ESI^+) calcd for $\text{C}_{31}\text{H}_{26}\text{N}_2\text{PdS} + \text{H}$ 565.0936, found 565.0945.

[9,18-Diethyl-8,19-dimethyl-24-thia-oxybenzporphyrinato]palladium(II) (25). A mixture of thiaoxybenzporphyrin **23**²⁷ (5.0 mg,

0.010 mmol) and palladium(II) acetate (5.0 mg, 0.022 mmol) in acetonitrile (5 mL) and chloroform (5 mL) was stirred under reflux for 20 min. The reaction was worked up as described above, and the product was recrystallized from chloroform–methanol to give the organometallic derivative (4.2 mg, 0.072 mmol, 69%) as a dark solid, mp >300 °C; IR: $\nu_{\text{C=O}}$ 1627 cm^{-1} ; UV–vis (CHCl_3) λ_{max} (log ϵ) 368 (4.33), 389 (sh, 4.31), 507 (4.75), 622 (4.05), 673 nm (4.04); UV–vis (1% TFA– CHCl_3) λ_{max} (log ϵ) 315 (4.62), 380 (4.55), 497 nm (4.65); ^1H NMR (500 MHz, 323 K, CDCl_3) δ 1.61–1.65 (6H, 2 overlapping triplets, $2\times\text{CH}_2\text{CH}_3$), 3.14 (3H, s, 8- CH_3), 3.23 (3H, s, 19- CH_3), 3.51–3.59 (4H, m, 9,18- CH_2), 7.07 (1H, d, $J = 9.0$ Hz, 3-H), 8.23 (1H, d, $J = 9.0$ Hz), 8.89 (1H, s, 6-H), 8.94 (1H, d, $J = 5.0$ Hz, 14-H), 8.99 (1H, d, $J = 5.0$ Hz, 13-H), 9.63 (1H, s, 16-H), 9.71 (1H, s, 11-H); ^{13}C NMR (125 MHz, 323 K, CDCl_3) δ 11.5 (8- CH_3), 11.8 (19- CH_3), 17.1, 17.3 ($2\times\text{CH}_2\text{CH}_3$), 20.1 (8,19- CH_2), 109.9 (16-CH), 111.8 (11-CH), 122.5, 123.8 (21-CH), 125.4, 126.4 (6-CH), 127.6 (3-CH), 130.2 (14-CH), 131.5 (13-CH), 134.5, 137.0, 137.3, 139.6, 139.7, 140.4, 140.7, 142.4, 142.7, 145.7, 148.1, 149.5 (4-CH), 188.0 (C=O); HRMS (ESI^+) calcd for $\text{C}_{28}\text{H}_{24}\text{N}_2\text{OPdS} + \text{H}$ 543.0727, found 543.0737.

2,4,13,15-Tetramethoxy-3,14-dimethyl-6,11,17,22-tetraphenyl-*opp*-dibenziporphyrin (32b). Nitrogen was bubbled through a solution of dimethoxybenzitrpyrrane **15b** (135 mg, 0.29 mmol) and dicarbinol **12b**¹⁵ (105 mg, 0.29 mmol) in chloroform (35 mL) for 10 min. A 10% $\text{BF}_3\cdot\text{Et}_2\text{O}$ solution in chloroform (200 μL) was added (turning the solution a light orange), and the solution was stirred under nitrogen protected from light for 2 h. DDQ (132 mg, 0.58 mmol) was added, and the reaction was allowed to stir for a further 5 min. Upon addition of DDQ, the reaction mixture instantly turned dark red. The solution was washed with water, and the solvent was evaporated under reduced pressure. The dark residue was chromatographed on grade 3 neutral alumina, eluting with dichloromethane. A bright yellow band was collected, and the solvent was evaporated under reduced pressure. The resulting solid was recrystallized from chloroform–methanol to yield the dibenziporphyrin (40 mg, 0.051 mmol, 18%) as an orange powder, 294–296 °C dec; UV–vis (1% $\text{Et}_3\text{N}-\text{CHCl}_3$) λ_{max} (log ϵ) 420 nm (4.58); ^1H NMR (500 MHz, CDCl_3) δ 2.06 (6H, s, 3,14- CH_3), 3.37 (12H, s, $4\times\text{OCH}_3$), 6.45 (2H, br s, $2\times\text{NH}$), 6.92 (4H, d, $J = 1.6$ Hz, 8,9,19,20-H), 7.18–7.22 (12H, m, *o*- and *p*-Ph), 7.31 (8H, t, $J = 7.6$ Hz, *m*-Ph), 7.62 (2H, s, 23,25-H); ^{13}C NMR (125 MHz, CDCl_3) δ 10.4 (3,14- CH_3), 60.4 ($4\times\text{OCH}_3$), 110.3, 126.2 (*p*-Ph), 126.8, 128.2 (*m*-Ph), 128.7 (8,9,19,20-CH), 129.07, 129.15 (*o*-Ph), 134.2 (23,25-CH), 142.0, 142.9, 158.6; HRMS (ESI^-) calcd for $\text{C}_{54}\text{H}_{46}\text{N}_2\text{O}_4 - \text{H}$ 785.3379, found 785.3379.

2,4,13,15-Tetramethoxy-6,11,17,22-tetraphenyl-*opp*-dibenziporphyrin (32a). Under the foregoing reaction conditions, benzitrpyrrane **15a** (132 mg, 0.29 mmol) was reacted with dicarbinol **12a**¹⁵ (103 mg, 0.29 mmol) to produce the dibenziporphyrin (31 mg, 0.041 mmol, 14%) as an orange powder, 266–268 °C dec; UV–vis (1% $\text{Et}_3\text{N}-\text{CHCl}_3$) λ_{max} (log ϵ) 422 nm (4.76); ^1H NMR (500 MHz, C_6D_6) δ 2.92 (12H, s, $4\times\text{OCH}_3$), 5.72 (2H, s, 3,14-CH), 6.51 (2H, s, $2\times\text{NH}$), 6.95 (4H, d, $J = 1.4$ Hz, 8,9,19,20-H), 7.09 (4H, t, $J = 7.4$ Hz, *p*-Ph), 7.24 (8H, t, $J = 7.5$ Hz, *m*-Ph), 7.52–7.55 (10H, overlapping doublet and singlet, *o*-Ph and 23,25-H); ^{13}C NMR (125 MHz, C_6D_6) δ 54.9 ($4\times\text{OCH}_3$), 98.4 (3,14-CH), 110.2, 121.8, 125.6 (*p*-Ph), 128.5 (*m*-Ph), 128.8 ($4\times\text{pyrrole-CH}$), 129.3 (*o*-Ph), 137.1 (23,25-CH), 143.0, 143.5, 159.2; HRMS (ESI^+) calcd for $\text{C}_{52}\text{H}_{42}\text{N}_2\text{O}_4$ 758.3139, found 758.3146.

2,4,13,15-Tetramethoxy-3-methyl-6,11,17,22-tetraphenyl-*opp*-dibenziporphyrin (32c). Under the foregoing reaction conditions, dimethoxybenzitrpyrrane **15b** (135 mg, 0.29 mmol) was reacted with dimethoxybenzene dicarbinol **12a**¹⁵ (103 mg, 0.29 mmol) to produce the dibenziporphyrin (29 mg, 0.038 mmol, 13%) as an orange powder, mp 272–274 °C; UV–vis (1% $\text{Et}_3\text{N}-\text{CHCl}_3$) λ_{max} (log ϵ) 421 nm (4.79); ^1H NMR (500 MHz, CDCl_3) δ 2.04 (3H, s, 3- CH_3), 3.42 (6H, s), 3.49 (6H, s) ($4\times\text{OCH}_3$), 6.42 (1H, br s, $2\times\text{NH}$), 6.46 (1H, s, 14-H), 6.90–6.94 (4H, m, 8,9,19,20-H), 7.15–7.22 (12H, m), 7.26–7.31 (8H, m) ($4\times\text{Ph}$), 7.65 (1H, s), 7.74 (1H, s) (23,25-H); ^{13}C NMR (125 MHz, C_6D_6) 10.2, 55.0, 59.7, 99.7, 110.4, 110.6, 121.9,

125.8, 126.0, 128.89, 128.95, 129.3, 129.5, 134.7, 136.5, 142.6, 143.0, 143.2, 143.3, 159.0, 159.3; HRMS (ESI^+) calcd for $\text{C}_{53}\text{H}_{44}\text{N}_2\text{O}_4$ 772.3296, found 772.3294.

■ ASSOCIATED CONTENT

Supporting Information

Tables and figures giving Cartesian coordinates and HOMO and LUMO surfaces, details of the crystallographic studies, and selected ^1H NMR, $^1\text{H}-^1\text{H}$ COSY, HSQC, DEPT-135, ^{13}C NMR, IR, and UV–vis spectra. This material is available free of charge via the Internet at <http://pubs.acs.org>.

■ AUTHOR INFORMATION

Corresponding Author

*tdlash@ilstu.edu

Notes

The authors declare no competing financial interest.

■ ACKNOWLEDGMENTS

The authors thank D. I. AbuSalim for carrying out the DFT and NICS calculations. This work was supported by the National Science Foundation under grant no. CHE-1212691, and the Petroleum Research Fund, administered by the American Chemical Society. The authors also thank NSF-CHE (grant no. 1039689) for funding the X-ray diffractometer.

■ REFERENCES

- (1) Lash, T. D.; Chaney, S. T.; Richter, D. T. *J. Org. Chem.* **1998**, *63*, 9076–9088.
- (2) Stepien, M.; Latos-Grazynski, L. *Acc. Chem. Res.* **2005**, *38*, 88–98.
- (3) Berlin, K.; Breitmaier, E. *Angew. Chem., Int. Ed. Engl.* **1994**, *33*, 1246–1247.
- (4) Lash, T. D. *Angew. Chem., Int. Ed. Engl.* **1995**, *34*, 2533–2535.
- (5) Stepien, M.; Latos-Grazynski, L. *Chem.—Eur. J.* **2001**, *7*, 5113–5117.
- (6) Lash, T. D.; Yant, V. R. *Tetrahedron* **2009**, *65*, 9527–9535.
- (7) Stepien, M.; Latos-Grazynski, L. *J. Am. Chem. Soc.* **2002**, *124*, 3838–3839.
- (8) Stepien, M.; Latos-Grazynski, L.; Szterenber, L.; Panek, L.; Latajka, Z. *J. Am. Chem. Soc.* **2004**, *126*, 4566–4580.
- (9) Lash, T. D.; Young, A. M.; Rasmussen, J. M.; Ferrence, G. M. *J. Org. Chem.* **2011**, *76*, 5636–5651.
- (10) Stepien, M.; Latos-Grazynski, L. *Org. Lett.* **2003**, *5*, 3379–3381.
- (11) Hung, C.-H.; Chang, F.-C.; Lin, C.-Y.; Rachlewicz, K.; Stepien, M.; Latos-Grazynski, L.; Lee, G.-H.; Peng, S.-M. *Inorg. Chem.* **2004**, *43*, 4118–4120.
- (12) Hung, C.-H.; Chang, G.-F.; Kumar, A.; Lin, G.-F.; Luo, L.-Y.; Ching, W.-M.; Diao, E. W.-G. *Chem. Commun.* **2008**, 978–980.
- (13) Huang, C.; Li, Y.; Yang, J.; Cheng, N.; Liu, H.; Li, Y. *Chem. Commun.* **2010**, *46*, 3161–3163.
- (14) Richter, D. T.; Lash, T. D. *Tetrahedron* **2001**, *57*, 3659–3673.
- (15) (a) Szymanski, J. T.; Lash, T. D. *Tetrahedron Lett.* **2003**, *44*, 8613–8616. (b) Lash, T. D.; Szymanski, J. T.; Ferrence, G. M. *J. Org. Chem.* **2007**, *72*, 6481–6492.
- (16) El-Beck, J. A.; Lash, T. D. *Org. Lett.* **2006**, *8*, 5263–5266.
- (17) (a) Miyake, K.; Lash, T. D. *Chem. Commun.* **2004**, 178–179. (b) Lash, T. D.; Miyake, K.; Xu, L.; Ferrence, G. M. *J. Org. Chem.* **2011**, *76*, 6295–6308.
- (18) Lash, T. D.; Pokharel, K.; Serling, J. M.; Yant, V. R.; Ferrence, G. M. *Org. Lett.* **2007**, *9*, 2863–2866.
- (19) (a) Mysliborski, R.; Latos-Grazynski, L. *Eur. J. Org. Chem.* **2005**, 5039–5048. (b) Mysliborski, R.; Latos-Grazynski, L.; Szterenber, L. *Eur. J. Org. Chem.* **2006**, 3064–3068.
- (20) Lash, T. D.; Toney, A. M.; Castans, K. M.; Ferrence, G. M. *J. Org. Chem.* **2013**, *78*, 9143–9152.

- (21) Results presented in part at the 247th ACS National Meeting, Dallas, Texas, March 2014 : Fosu, S. C.; Lash, T. D. *Abstracts of Papers*, ORGN-677.
- (22) AbuSalim, D. I.; Lash, T. D. *Org. Biomol. Chem.* **2014**, *12*, 8719–8736.
- (23) Lash, T. D. *Chem.—Asian J.* **2014**, *9*, 682–705.
- (24) (a) Stilts, C. E.; Nelen, M. I.; Hilmey, D. G.; Davies, S. R.; Gollnick, S. O.; Oseroff, A. R.; Gibson, S. L.; Hilf, R.; Detty, M. R. *J. Med. Chem.* **2000**, *43*, 2403–2410. (b) Hilmey, D. G.; Abe, M.; Nelen, M. I.; Stilts, C. E.; Baker, G. A.; Baker, S. N.; Bright, F. V.; Davies, S. R.; Gollnick, S. O.; Oseroff, A. R.; Gibson, S. L.; Hilf, R.; Detty, M. R. *J. Med. Chem.* **2002**, *45*, 449–461.
- (25) Schleyer, P. v. R.; Maerker, C.; Dransfeld, A.; Jiao, H.; Hommes, N. J. R. v. E. *J. Am. Chem. Soc.* **1996**, *118*, 6317–6318.
- (26) Wells, P. R. *Chem. Rev.* **1963**, *63*, 171–219.
- (27) (a) Liu, D.; Lash, T. D. *Chem. Commun.* **2002**, 2426–2427. (b) Liu, D.; Ferrence, G. M.; Lash, T. D. *J. Org. Chem.* **2004**, *69*, 6079–6093.
- (28) Jain, P.; Ferrence, G. M.; Lash, T. D. *J. Org. Chem.* **2010**, *75*, 6563–6573.
- (29) Venkatraman, S.; Anand, V. G.; Pushpan, S. K.; Sankar, J.; Chandrashekar, T. K. *Chem. Commun.* **2002**, 462–463.
- (30) Berlicka, A.; Dutka, P.; Szterenber, L.; Latos-Grazynski, L. *Angew. Chem., Int. Ed.* **2014**, *53*, 4885–4889.
- (31) Cremer, D.; Pople, J. A. *J. Am. Chem. Soc.* **1975**, *97*, 1354–1358.
- (32) Allen, F. H. *Acta Crystallogr.* **2002**, *B58*, 380–388.
- (33) Linstead, R. P. *J. Chem. Soc.* **1953**, 2873–2884.
- (34) Clark, P. F.; Elvidge, J. A.; Linstead, R. P. *J. Chem. Soc.* **1954**, 2490–2497.
- (35) (a) Wu, R.; Cetin, A.; Durfee, W. S.; Ziegler, C. J. *Angew. Chem., Int. Ed.* **2006**, *45*, 5670–5673. (b) Cetin, A.; Sripothongnak, S.; Kawa, M.; Durfee, W. S.; Ziegler, C. J. *Chem. Commun.* **2007**, 4289–4290. (c) Sripothangnok, S.; Barone, N.; Ziegler, C. J. *Chem. Commun.* **2009**, 4584–4586.
- (36) Ziegler, C. J. In *Handbook of Porphyrin Science with Applications to Chemistry, Physics, Materials Science, Engineering, Biology and Medicine*; Kadish, K. M.; Smith, K. M.; Guillard, R., Eds.; World Scientific Publishing: Singapore, 2012; Vol. 12, pp 114–238.
- (37) AbuSalim, D. I.; Merfeld, M. L.; Lash, T. D. *J. Org. Chem.* **2013**, *78*, 10360–10368.
- (38) Sessler, J. L.; Cho, W.-S.; Lynch, V.; Kral, V. *Chem.—Eur. J.* **2002**, *8*, 1134–1143.
- (39) Tardieux, C.; Bolze, F.; Gros, C. P.; Guillard, R. *Synthesis* **1998**, 267–268.
- (40) Li, R.; Lammer, A. D.; Ferrence, G. M.; Lash, T. D. *J. Org. Chem.* **2014**, *79*, 4078–4093.